Article

New Insight into Sperm Capacitation: A Novel Mechanism of 17β-Estradiol Signalling

Tereza Bosakova [1], Antonin Tockstein [1], Natasa Sebkova [2], Ondrej Simonik [2,3],
Hana Adamusova [1], Jana Albrechtova [4,5], Tomas Albrecht [4,5], Zuzana Bosakova [1,*] and
Katerina Dvorakova-Hortova [2,4,*]

[1] Department of Analytical Chemistry, Faculty of Science, Charles University, Albertov 2030, 128 43 Prague, Czech Republic; terezabosakova@seznam.cz (T.B.); atockstein@seznam.cz (A.T.); hana.adamusova@gmail.com (H.A.)

[2] Laboratory of Reproductive Biology, Institute of Biotechnology CAS, v.v.i., BIOCEV, Prumyslova 595, 252 50 Vestec, Czech Republic; Natasa.Sebkova@ibt.cas.cz (N.S.); simoniko@af.czu.cz (O.S.)

[3] Department of Veterinary Sciences, Faculty of Agrobiology, Food and Natural Resources Czech University of Life Sciences Prague, Kamycka 129, 165 00 Prague, Czech Republic

[4] Department of Zoology, Faculty of Science, Charles University, Vinicna 7, 128 44 Prague, Czech Republic; jana.brehova@seznam.cz (J.A.); albrecht@ivb.cz (T.A.)

[5] Institute of Vertebrate Biology, v.v.i., Czech Academy of Sciences, Kvetna 8, 603 65 Brno, Czech Republic

* Correspondence: bosakova@natur.cuni.cz (Z.B.); katerina.hortova@ibt.cas.cz (K.D.-H.);
Tel.: +420-22-195-1231 (Z.B.); +420-32-587-3799 (K.D.-H.)

check for
updates

Abstract: 17β-estradiol (estradiol) is a natural estrogen regulating reproduction including sperm and egg development, sperm maturation—called capacitation—and sperm–egg communication. High doses can increase germ cell apoptosis and decrease sperm count. Our aim was to answer the biological relevance of estradiol in sperm capacitation and its effect on motility and acrosome reaction to quantify its interaction with estrogen receptors and propose a model of estradiol action during capacitation using kinetic analysis. Estradiol increased protein tyrosine phosphorylation, elevated rate of spontaneous acrosome reaction, and altered motility parameters measured Hamilton-Thorne Computer Assisted Semen Analyzer (CASA) in capacitating sperm. To monitor time and concentration dependent binding dynamics of extracellular estradiol, high-performance liquid chromatography with tandem mass spectrometry was used to measure sperm response and data was subjected to kinetic analysis. The kinetic model of estradiol action during sperm maturation shows that estradiol adsorption onto a plasma membrane surface is controlled by Langmuir isotherm. After, when estradiol passes into the cytoplasm, it forms an unstable adduct with cytoplasmic receptors, which display a signalling autocatalytic pattern. This autocatalytic reaction suggests crosstalk between receptor and non-receptor pathways utilized by sperm prior to fertilization.

Keywords: 17β-estradiol; sperm; capacitation; acrosome reaction; kinetics; autocatalysis; HPLC MS/MS; CASA

1. Introduction

In order for mammalian sperm to fertilize, it must undergo a series of maturation events in the female reproductive tract, called capacitation [1]. In general, capacitation involves membrane rearrangement, cholesterol efflux, activation of specific signal transduction pathways leading to protein tyrosine phosphorylation (TyrP), and cytoskeleton rearrangements [2–4]. As much as capacitation-related increase of TyrP has been postulated to be a key capacitation marker [1,3], a study [5] showed that this may not be an essential event in mouse sperm, and lack of TyrP can

be bypassed in vivo by an as yet unknown mechanism. Therefore, it is important to evaluate the status of capacitation by other parameters, such as motility and sperm ability to undergo acrosome reaction (AR). Hamilton-Thorne Computer-Aided Sperm Analysis (CASA) is generally used for the monitoring of sperm motility and provides a set of standard kinematic parameters that aids with the identification of changes in trajectories and flagellar beating patterns connected with hyperactivation as an important part of sperm capacitation [6,7]. In vivo capacitation occurs mainly in the uterus and oviducts, facilitated by substances in the female genital tract including estrogen. It has been demonstrated that endocrine disruptors, including estrogen, significantly modulate capacitation in vitro and can also increase its speed [8–12]. Estradiol and its analogues induced not only capacitation but also non-induced (spontaneous) AR [13]. Progesterone-induced AR [9,13], progesterone-enhanced sperm hyperactivation [14–16], and progesterone-increased TyrP [14,15] are all suppressed by estradiol.

Estrogen cell signalling is a crucial event, and both general and sperm specific mechanisms are still not understood. An interaction between the most influential of estrogen, estradiol and its estrogen receptors (ERs), has been described through nuclear receptors (nER) and membrane (mER) and cytoplasmic (cER) receptors [17,18]. These receptors might be either of the same composition, just translocated from the nucleus to the membrane [19,20], or they may represent a novel kind of ERs [21–23]. In addition to the estrogen-based receptors, the ability of non-ER membrane-associated proteins to bind and transfer estradiol across the plasma membrane (PM) has been described [24]. On the top of the transportation receptors, estradiol is able to penetrate and pass through the PM without any help [25,26]. The complexity of the system is stressed by two routes of estradiol action: the slow genomic and the rapid non-genomic routes. The generally excepted model is built on the binding of the intracytoplasmic estradiol to the well-described and understood nER, targeting DNA sequences known as estrogen response elements (EREs) [27] or DNA-binding transcription factors [28–30], both leading to transcriptional activation of the associated genes [31,32]. The genomic pathway requires cell transcriptional activity and time, none of which these mature spermatozoa possess. In this case, the non-genomic pathway remains the only option for sperm in order to regulate the signalling pathways that are crucial for the capacitation processes. For obvious reasons, it is difficult to study capacitation in vivo; therefore, it is crucial to understand precise in vitro conditions, including dynamics, speed, and amount of exogenous estrogen that is bound to sperm receptors during capacitation. Importantly, there has been reported genetic variation between mouse strains, which play a role in fertility success and sperm quality [33–35]. Therefore, strain specific differences also need to be addressed.

The mathematical interpretations and general quantified process dynamics bring another perspective to help explain this crucial biological event. In a previous study [36], the mathematical theory for the mechanism when sperm maturation ability is amended by external stimuli [37] was proposed. It was shown that the chemical kinetics can be applied to sperm in the role of reactant and that kinetic analysis could be a useful tool for monitoring and predicting the specific molecular mechanisms involved in certain biological signalling pathways. Kinetic analysis data can serve as a tool for predicting the general hormone-receptor mechanism and provide new insights into the selected biological reaction. At the moment, the scientific community knowledge has extended to the description of individual signalling scenarios in both somatic and male germinal cells, but the mechanism of the action remains unknown.

The objectives of this study were as follows: (1) to clarify the effect of estradiol on sperm capacitation, motility, and acrosome reaction; (2) to develop a sensitive analytical high-performance liquid chromatographic method with tandem mass spectrometric detection (HPLC-MS/MS) for the determination of total unbound estradiol concentration in the sperm capacitation in vitro; and (3) to reveal whether the concentration of estradiol versus the time of ongoing capacitation fits an equation or a system of equations of chemical kinetics. By applying kinetic analysis to our data obtained by HPLC-MS/MS, and measuring the estradiol dynamics during mouse sperm capacitation, we propose a unique type of autocatalytic estradiol signalling, which could unify all the estradiol actions into one complex event.

2. Results

2.1. Monitoring of Estradiol Concentration during Capacitation In Vitro by HPLC

One of the key compounds of the culture media used for in vitro capacitation is bovine serum albumin (BSA), which is responsible for the transfer of cholesterol and phospholipids from the plasma membrane bilayer and is essential for sperm capacitation [1,3,38,39]. In order to monitor the effects of estradiol on sperm capacitation in vitro, it was essential to determine how much estradiol, added into commercial culture media for in vitro sperm capacitation and fertilization (M2 medium, Sigma-Aldrich, Darmstadt, Germany), is available for sperm as the process of binding of estradiol to BSA is known [40]. This was determined for all three tested estradiol concentrations 200, 20, and 2 µg/L (730, 73, and 7.3 nM, respectively) after one hour of in vitro sperm incubation in M2 medium at 37 °C and 5% CO_2. These calculated values were taken as the initial concentrations at capacitation time 0 and the dependencies of total unbound estradiol concentration on capacitation time were measured. The process of capacitation was monitored in the time range of 0 to 180 min with a 30-min interval between sample collection. Extending the time to over 180 min had no physiological relevance, as the capacitation of mouse sperm in vivo is achieved within 90 min (180 min at the latest). In order to cover genetic variation between mouse strains, we performed all the experiments for a laboratory inbred albino (BALB/c) and black (C57BL/6Nvel) house mouse strains and compared the results (Figure 1).
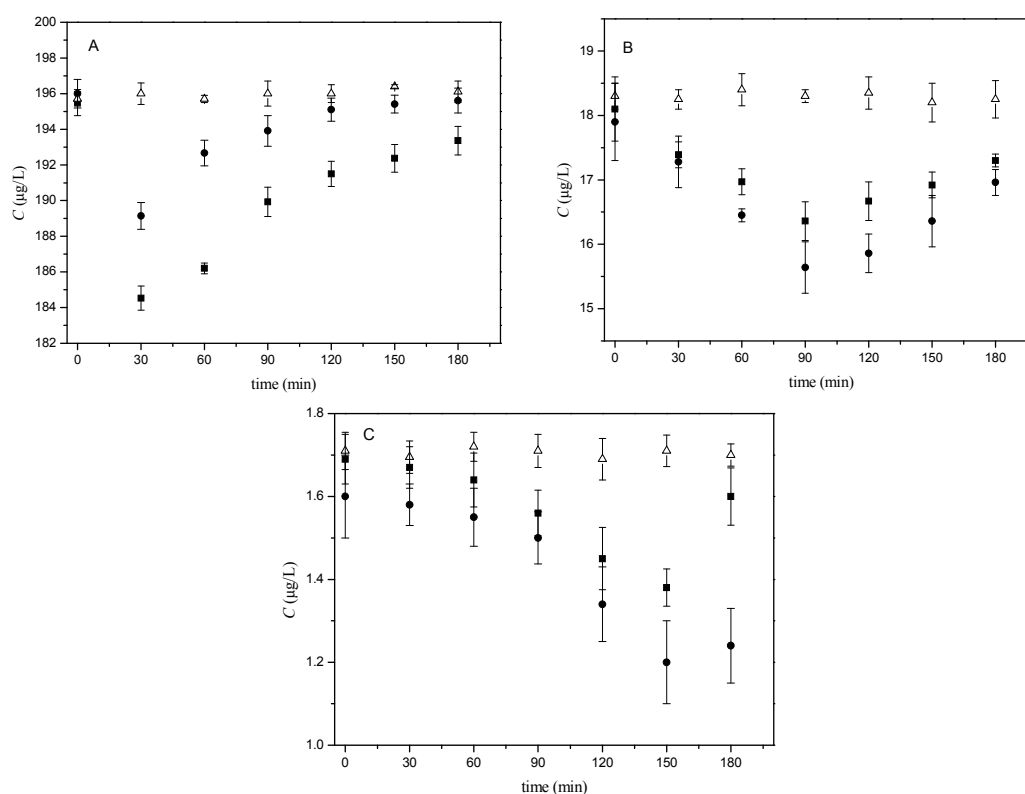

Figure 1. Dependencies of the concentration of total unbound estradiol on the time of mouse sperm capacitation in vitro. The tested concentrations of estradiol in M2 medium were (**A**) 200 µg/L, (**B**) 20 µg/L, and (**C**) 2 µg/L. Each experiment was carried out for samples with added mouse sperm (solid circles for BALB/c sperm, solid squares for C57BL/6Nvel sperm) and for reference samples without sperm (blanks, open triangles). The samples were prepared in three parallel sets, where each set represented sperm collecting from one individual; each sample was measured in five replicates; experimental conditions: 50/50 (*v/v*) acetonitrile (ACN)/H_2O, both containing 0.1% HCOOH, measured in multiple reaction monitoring (MRM) mode for transition 255.2 to 158.9; error bars were calculated using the standard deviations (*n′* = 3). For details, see Sections 4.2 and 4.3 and Table A1 in Appendix B (Supplementary Materials).

As can be seen from Figure 1A–C, all the tested estradiol concentrations in blank samples remain practically constant (open triangles) during capacitation. For samples with the addition of sperm (solid circles and squares), similar trends were obtained for all the tested concentrations (200, 20, and 2 µg/L) and both spermatozoa of BALB/c or C57BL/6Nvel mouse laboratory strains. In general, the concentration of total unbound estradiol decreases to reach its minimum and then increases again. However, the position of the minimum differs for the individual tested estradiol concentrations. For the starting concentration 200 µg/L (Figure 1A) the straightforward decrease occurred at the beginning of capacitation time within 0–30 min. The drop of 20 µg/L at the starting concentration can be observed later at 60–90 min (Figure 1B) and the dependence obtained for starting concentration 2 µg/L exhibited its minimum between 150–180 min (Figure 1C). Only slightly different extents of decline were observed between two different strain origins of spermatozoa within the individually tested estradiol concentration (solid circles for BALB/c sperm versus solid squares for C57BL/6Nvel sperm).

Analogical measurements were run under non-capacitating conditions using a medium without BSA. No differences between the samples and blanks were observed for the dependencies of total unbound estradiol concentrations on incubation time (0–180 min) and the estradiol concentrations remained constant up to 180 min.

2.2. Kinetic Analysis

Given that kinetic analysis has already been successfully used for analysis of data describing the reduced capacitation ability of sperm [36], it was also used to analyse the reaction of sperm with estradiol. The course of a sperm response on the added estradiol (Figure 1) indicated an autocatalytic character with a formation of an unstable adduct followed by its decomposition. Therefore, these results were subjected to kinetic analysis. For a better comparison of the measured time-dependent concentrations of total unbound estradiol (C), the relative concentrations of total unbound estradiol (B) were introduced defined as $B_t = C_t/C_{t=0}$, where B_t is the relative concentration of total unbound estradiol calculated for the capacitation times (0–180 min), C_t is the concentration of total unbound estradiol measured at capacitation times (30–180 min) and $C_{t=0}$ is the concentration of total unbound estradiol measured at capacitation time 0 min. Calculated B_t values for BALB/c and C57BL/6Nvel mouse strains are given in Table 1.

Table 1. Relative concentrations of total unbound estradiol (B_t) calculated from the measured time-dependent concentrations of total unbound estradiol (C) (Figure 1A–C) obtained during capacitation for three tested estradiol concentrations and two inbreed mouse strains; mean $\pm$ standard error of the mean.

Capacitation Time (min)	B_t					
	200 µg/L		20 µg/L		2 µg/L	
	BALB/c	C57BL/6N	BALB/c	C57BL/6N	BALB/c	C57BL/6N
0	1.000 ± 0.003	1.000 ± 0.003	1.000 ± 0.028	1.000 ± 0.023	1.000 ± 0.050	1.000 ± 0.070
30	0.965 ± 0.005	0.944 ± 0.004	0.965 ± 0.033	0.958 ± 0.024	0.987 ± 0.055	0.988 ± 0.073
60	0.983 ± 0.004	0.952 ± 0.003	0.919 ± 0.026	0.938 ± 0.024	0.969 ± 0.061	0.982 ± 0.079
90	0.989 ± 0.005	0.968 ± 0.005	0.874 ± 0.031	0.904 ± 0.025	0.938 ± 0.055	0.923 ± 0.071
120	0.995 ± 0.004	0.979 ± 0.004	0.886 ± 0.028	0.921 ± 0.025	0.838 ± 0.046	0.858 ± 0.069
150	0.997 ± 0.004	0.984 ± 0.005	0.914 ± 0.032	0.929 ± 0.023	0.751 ± 0.062	0.826 ± 0.066
180	0.998 ± 0.005	0.989 ± 0.005	0.958 ± 0.028	0.956 ± 0.022	0.773 ± 0.058	0.947 ± 0.074

The suggested kinetic schema was described by kinetic products and rate constants in the form of rate equations. Relative values for individual variables were introduced. The system of differential equations was solved by numerical integration with the simultaneous optimization of the rate constants used to calculate the theoretical B_t values. Using MATLAB software, optimal parameters (overall rate constants K_2, K_3 and molar ratio n) were determined by searching the minimum of absolute values of the difference between theoretical and experimental B_t values (Table 2). These values

were then used for the design of the theoretical $B(t)$ curves. The fit of the theoretical $B(t)$ curves and experimentally obtained data is shown in Figure 2. For a detailed description of mathematical procedure, see Appendix A (Supplementary Materials).
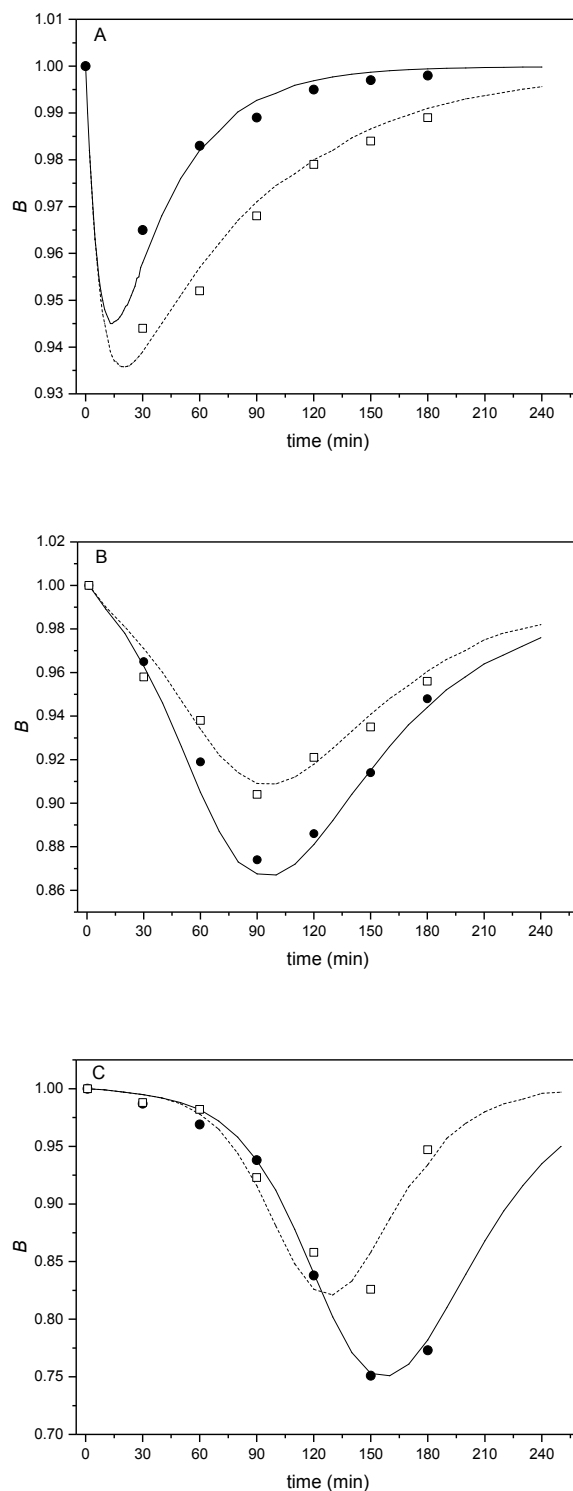

Figure 2. Theoretical shape of the $B(t)$ curves (solid line for BALB/c, dashed line for C57BL/6Nvel) obtained by integration of kinetic equations (details in Appendix A in Supplementary Materials) for the selected dilution D, molar ratio n, and optimized values of K_2 and K_3 (Table 2) with designation of the points obtained in the experiment (solid circles for the BALB/c experiments, and solid squares for the C57BL/6Nvel experiments) for estradiol concentrations; (**A**) 200 μg/L, (**B**) 20 μg/L, and (**C**) 2 μg/L.

Table 2. Calculated constants for three tested estradiol concentrations and two inbreed mouse strains, where D is dilution factor, n is molar ratio, and K_2 and K_3 are overall rate constants.

Constants	200 µg/L		20 µg/L		2 µg/L	
	BALB/c	C57BL/6N	BALB/c	C57BL/6N	BALB/c	C57BL/6N
D	1	1	0.1	0.1	0.01	0.01
n	12	12	1.2	1.2	0.12	0.12
K_2	4.0	2.0	4.5	4.0	4.5	5.5
K_3	3.0	1.3	4.3	6.0	3.5	6.5

Referring to Figure 2, the experimental points fit the theoretical $B(t)$ curves well for both tested mouse strains. Firstly, the tangent slope of these curves increases, which means that the reaction between estradiol and cytoplasmic receptors accelerates and the formation of their adduct ($E2/cER$) takes place autocatalytically. The minima appeared at times t_{min} through the formation and subsequent decomposition of the adduct. An important feature of the $B(t)$ curves is a considerable shift in t_{min} with decreasing estradiol concentration (200 $\rightarrow$ 2 µg/L). The kinetic analysis showed that the initial adsorption at specific membrane centres (Langmuir adsorption isotherm) is a prerequisite for an autocatalytic reaction associated with gradual increase in membrane fluidity in the formation of an adduct (signalling process). The position of t_{min} in relation to the time at 10-fold and 100-fold dilution of the highest employed concentrations of estradiol (200 µg/L), i.e., 1/10 or 1/100 of the added amount of estradiol, indicates that the reaction of estradiol with the sperm receptors does not have an integral order because the position of t_{min} would not change for first-order but would change 10-fold for a second-order reaction (Appendix A in Supplementary Materials).

A slight shift was observed between the theoretical curves reflecting differences in estradiol binding dynamics between two mouse inbreed strains, BALB/c and C57BL/6Nvel, supporting the strain/sub-strain-specific phenotypic responses for mice of different genetic backgrounds, which is also reflected in the fertilizing ability of sperm [33]. However, the theoretical curves $B(t)$ fit the experimental points for both tested types of mice with the same outcome, which supports the evidence of finding the theoretical mechanism, which fits to differences between mouse strains. The shift in experimental data may be related to the fact that C57BL/6Nvel mice have lower fertility efficiency [34] and sperm motility parameters, such as reaching the hyperactivated stage the sperm capacitation [35].

2.3. Capacitation Status Monitored by TyrP

During capacitation, signalling pathways are activated resulting in protein phosphorylation, especially on tyrosine (Tyr) residues, which are the key marker of successfully ongoing capacitation process [3]. In order to monitor capacitation status and see whether estradiol kinetics changes under conditions that do not support capacitation, a series of experiments monitoring time-dependent (0, 60, and 90 min) sperm protein TyrP in absence (control) or presence of estradiol under capacitating (Figure 3) and non-capacitating (Figure 4) conditions were run. The presence of BSA in the medium is essential for binding cholesterol from the sperm plasma membrane, which consequently results in the signalling pathway activation and leads to the initiation of sperm capacitation. This cascade of events does not happen in the absence of BSA [1,3,41]. We monitored the time-dependent sperm protein TyrP using Western blot (WB) protein analysis (Figures 3 and 4) and immunofluorescence detection (Figure A1, Appendix B in Supplementary Materials).

The results of WB analysis showed differences in the amount of protein TyrP between the control samples (Figure 3) and sperm that were incubated in BSA-absent medium (Figure 4). The results show that, during sperm capacitation, a typical increase in the number of proteins that were phosphorylated on tyrosine residues occurred, and TyrP was elevated when estradiol was added (Figure 3). These results correspond to previous findings [11,12]. TyrP no longer increased after 90 min of capacitation and remained steady thereafter (results not shown). In the absence of BSA in the medium (its precise composition as M2 except for BSA) (Figure 4), the protein detection did not show any increase in TyrP, and its level corresponded to the control time 0, when sperm capacitation was not initiated (Figure 3). We did not detect any rescue effect by estradiol addition. TyrP did not occur in that group either (Figure 4).
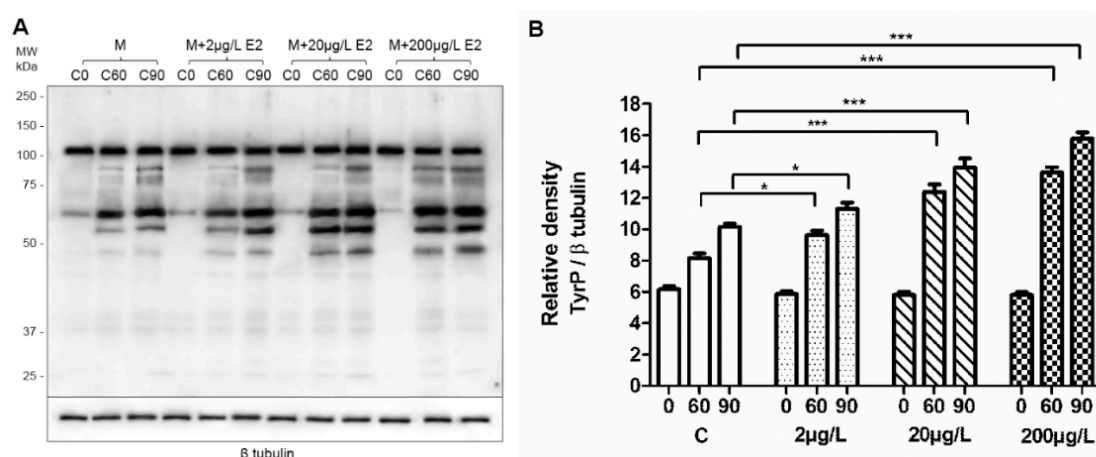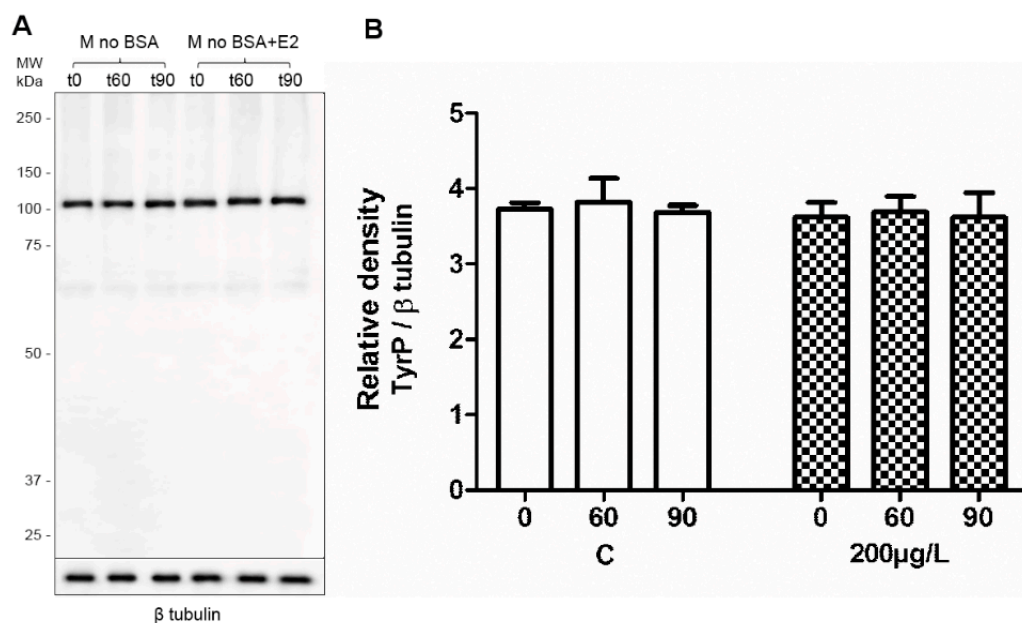

Figure 3. Time-dependent sperm protein TyrP in presence of estradiol (E2) under capacitating conditions as assessed by Western blot analysis and relative densitometry. (**A**) Control samples: sperm capacitating in commercial M2 medium (M); M + E2: the medium enriched by E2 in different concentrations (2, 20, and 200 µg/L). In contrast with freshly released epididymal sperm (t0), protein TyrP increased during sperm capacitation (t60, t90) with a maximum value at 90 min (t90). The protein TyrP was stronger when E2 was present. Increasing concentrations of E2 lead to stronger protein TyrP. β-tubulin was used as the loading control. The samples contained a protein equivalent of 106 cells. Five experiments per group were prepared; the representative results are shown. (**B**) Densitometry analysis of TyrP protein levels in sperm of control samples and sperm incubated in M2 medium enriched by E2. The densitometry analysis indicates relative levels of TyrP revealed a time-dependent and significant increase. Error bars indicate the SD. The statistical significance of the differences among protein TyrP abundances in different groups is indicated by asterisks (* $p < 0.05$, *** $p \leq 0.001$).

Sperm head protein TyrP plays a crucial role in sperm-*zona pellucida* (an extracellular matrix of the egg) recognition and its level is much lower (up to 15%) compared to complete sperm tail protein TyrP [42]. In order to evaluate TyrP sperm head proteins, sperm smears were assessed by immunofluorescence labelling. The graph showing the percentage of sperm head TyrP during sperm capacitation (Figure A1, Appendix B in Supplementary Materials) indicates an increasing level of TyrP reaching the highest values (approx. 15%) in 90 min of capacitation in the control. When estradiol was added at the beginning of sperm capacitation, the number of positive sperm heads raised to 20% within 90 min, which correlated to previously published work [11]. In contrast (Figure A1, Appendix B in Supplementary Materials), TyrP labelling was significantly lower (approx. 3%) in all samples where sperm were incubated in the medium without BSA, and the addition of estradiol did not provoke the sperm head protein TyrP. The TyrP values of the groups in absence of BSA statistically correspond to the non-capacitated sperm.

The results from WB agreed with those of fluorescence, even though WB reflects the level of whole sperm protein TyrP compared to fluorescence analysis, which only focused on sperm head status. The analysis proved that, in the medium without BSA, sperm capacitation does not occur, not even in the presence of estradiol, which, in capacitation conditions, increase the protein TyrP and do not promote the capacitation in non-capacitating conditions. For detailed information on methodology, please see Appendix A in Supplementary Materials.

Figure 4. Time-dependent sperm protein TyrP in presence of estradiol (E2) under non-capacitating conditions by Western blot analysis and relative densitometry. (**A**) Control samples: sperm capacitating in commercial M2 medium (M); M + E2: the medium enriched by E2 in different concentrations (2, 20, and 200 μg/L); M with no BSA; and M with no BSA + E2: sperm left in the medium without BSA or without BSA with the addition of E2 (200 μg/L) for 60 and 90 min. Increasing protein TyrP was not observed for any time (t60, t90) or experimental conditions. All incubation times and conditions indicate the same patterns that were identical to the non-capacitating sperm pattern (t0). β-tubulin was used as the loading control. The samples contained a protein equivalent of 106 cells. Five experiments per group were prepared, representative result shown. (**B**) Densitometry analysis of TyrP protein levels in sperm of control samples and sperm incubated in M2 medium enriched by E2 (200 μg/L). The densitometry analysis indicates the same patterns in all the incubation times and conditions. Error bars indicate the SD. There was no statistical significance among protein TyrP abundances in different groups.

2.4. Sperm Motility and Hyperactivation Measured by CASA

Linear mixed effects model with lateral head displacement (ALH) as the dependent variable indicated that estradiol concentrations affected strains in a different way (interaction term *concentration x strain* was significant: $\chi^2 = 11.29$, $\Delta Df = 3$, $p = 0.01$). Strains were therefore analyzed separately. ALH was, to some extent, affected by estradiol in C57BL/6Nvel (effect of estradiol concentration: $\chi^2 = 8.28$, $\Delta Df = 3$, $p = 0.041$) and increased compared to control in estradiol concentration 20 μg/L by 0.73 ± 0.25 (SE) μm. There was no effect of estradiol concentrations on ALH in BALB/c ($\chi^2 = 4.95$, $\Delta Df = 3$, $p = 0.19$) (Table A2, Appendix B in Supplementary Materials).

In curvilinear velocity (VLC), the interaction term *concentration x strain* was also significant (χ^2 = 10.676, ΔDf = 3, p = 0.014). Estradiol concentrations had a clear effect on sperm motility in BALB/c (effect of estradiol concentration: χ^2 = 16.35, ΔDf = 3, p < 0.001). VLC was reduced compared to the control, particularly at estradiol concentrations of 2 μg/L (reduction 12.78 $\pm$ 3.45 (SE) μm/s) and 20 μg/L (reduction 7.98 $\pm$ 3.45 (SE) μm/s). In contrast, the presence of estradiol had a weak negative, but insignificant, effect on C57BL/6Nvel (effect of estradiol concentration: χ^2 = 1.57, ΔDf = 3, p = 0.67; Table A2, Appendix B in Supplementary Materials). For detailed information on methodology, please see Appendix A in Supplementary Materials.

2.5. Acrosome Reaction

In order to monitor the capacitation outcome in connection to estradiol, the experiments were designed to compare the solitary effect of estradiol and its competing dose-dependent effect with progesterone during capacitation, as well as the effect of estradiol on induction of AR in relevance to progesterone after capacitation finished. The presence of estradiol from the beginning of capacitation had a stimulatory effect on the rate of spontaneous AR and was positively correlated with estradiol increasing concentration (Figure 5). In presence of both E2 and progesterone the percentage of sperm remained constant after the AR despite the expected stimulatory effect of a higher concentration of progesterone compared to estradiol. The AR remained the same between the control and experimental groups (Figure 6). The results were, however, different when sperm were exposed for 90 min to estradiol and progesterone only after completing capacitation. The AR was enhanced in the group of estradiol with progesterone. This was expected, as the progesterone concentration exceeded the concentrations of estradiol [15]; however, increasing the rate of AR was also positively correlated with increasing estradiol concentration (Figure 7), which was not the case when steroid hormones were added at the beginning of capacitation. For detailed information on methodology, please see Appendix A in Supplementary Materials.
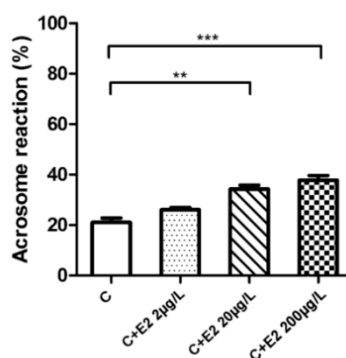

Figure 5. Acrosome reaction during 90 min capacitation (C) in presence of estradiol (E2). Sperm were capacitated in presence of E2 (C + E2 2; 20 and 200 μg/L) or without E2 (control, C). The rate of acrosome reaction (AR) was monitored by peanut agglutinin lectin (PNA). A dose-dependent increase in spontaneous AR during 90 min capacitation was demonstrated. A total of 200 cells were counted in six individual samples. The differences in percentage distribution of sperm with intact acrosome and acrosome reacted sperm was statistically analyzed. Error bars represent the SD. (** p < 0.01, *** p < 0.001).
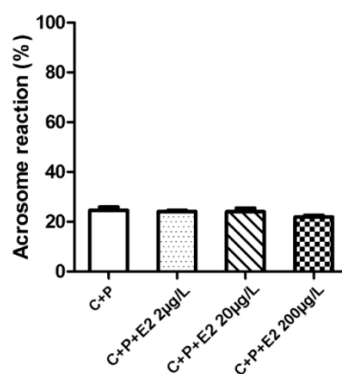
Figure 6. Acrosome reaction during 90 min capacitation (C) in simultaneous presence of estradiol (E2) and progesterone (P). Sperm were capacitated in capacitating medium in presence of progesterone (10 μM, 3144 μg/L) with E2 (C + P + E2: 2, 20, and 200 μg/L) or without E2 (control, C + P). A total of 200 cells were counted in six individual samples. No differences were detected in contrast with control samples. The AR rate was the same for all different experimental E2 concentrations. Error bars indicate the SD. There was no statistical significance among sperm incubations with different E2 concentrations.
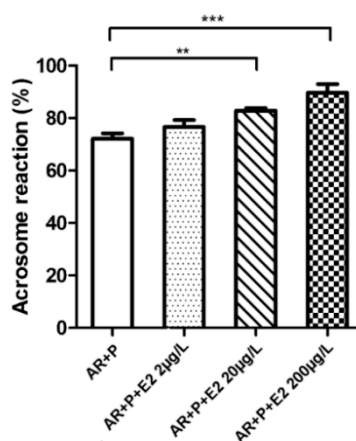

Figure 7. Acrosome reaction (AR) in presence of estradiol (E2) and progesterone (P). Sperm were capacitated (90 min) followed by progesterone (induced 10 μM) induced AR (90 min) in presence of E2 (AR + P + E2 2; 20 and 200 μg/L) or without E2 (control, AR + P). The results show an E2 dose-dependent increase in AR rate. A total of 200 cells were counted in six individual samples. Error bars indicate the SD. ** $p < 0.01$, *** $p \leq 0.001$.

3. Discussion

Estradiol concentration in follicular fluid is higher than in the reproductive female tract and comparable with our experimental concentrations [43]. Specifically, in female mammals, estradiol concentration in the ovarian fluid is at least two-fold higher compared with that of plasma [44], and it fluctuates during estrus, and between 145 and 2100 pg/mL for mouse and rat [45]. Therefore, sperm are expected to be exposed to high concentrations during certain stages of their capacitation in the female reproductive tract [43,46]. Based on these facts, the in vivo sperm exposure to estradiol is a common phenomenon. Understanding estradiol action is of importance because higher concentrations of estradiol than physiological concentrations were reported to lead to in vivo premature capacitation and a decreased fertilizing potential [12]. Sperm capacitation happens 30–90 min after introducing sperm to the female reproductive tract surroundings [3], but also depends on the estrogen concentration, which promotes a time dependent stimulatory effect and increased the protein TyrP in vitro [11] and altered the ability of sperm to undergo an induced acrosome reaction [11,13]. A recent study [5] showed that TyrP may not be essential for mouse sperm capacitation/fertilization in vivo, as an inability of tyrosine-protein kinase *Fer*DR/DR mice with a kinase-inactivation mutation to promote

TyrP did not result in sterility; however, their fertility outcome decreased. Our results showed that estradiol increased TyrP in capacitation sperm, the overall TyrP protein level, and the TyrP of the sperm head. It has been shown that sperm head TyrP is a crucial event prior to AR and only up to 15% of sperm reach this state [42]. Considering that decreased in vitro sperm fertility caused by absence of TyrP in mouse may be overcome simply by the interaction of sperm with the female reproductive environment [5], a hormonal player may be involved. Estradiol concentration is high in the site of sperm–egg interaction and may trigger alternative pathways or promote sperm fitness based on its inducible effect seen in the case of both sperm overall and head TyrP (Figure 3, Figure A1, Appendix B in Supplementary Materials).

In addition to the estradiol stimulatory effect on capacitation [8–12], the non-induced (spontaneous) AR was elevated [13]. The spontaneous acrosome reaction has been shown to be a physiological process in mouse sperm and can be completed before sperm reaches the *zona-pellucida* [47]. The acrosome reacted sperm are still able to fertilize the egg [48]; therefore, the stimulatory effect of estradiol (Figure 5) may be considered important for sperm fertilizing potential. In the presence of progesterone, the stimulatory effect of estradiol is abolished (Figure 6), which is correlated with estradiol-based suppression of progesterone-induced TyrP [14,15], hyperactivation [14–16], and AR [9,13]. This was not the case for spontaneous AR. The acrosome reaction is enhanced when the concentration of progesterone is dominant over estradiol, and when sperm are exposed to both steroid hormones simultaneously after completing the capacitation (Figure 7). However, spontaneous AR during capacitation remained constant (approx. 20%), despite the presence of progesterone and estradiol. When estradiol was present by itself from the beginning of capacitation, spontaneous AR was elevated, which allowed us to measure and quantify the induction effect of estradiol on sperm capacitation and deduce a potential mechanism of estradiol interaction with ERs.

To evaluate the relevance of the estradiol effect on sperm capacitation, we used CASA as powerful tool to monitor subtle specific changes in sperm motility. An additional process, called hyperactivation, occurs during sperm capacitation [49]. Hyperactivated spermatozoa are characterized by higher values of curvilinear velocity (VCL) and lateral head displacement (ALH) [35]. These changes in sperm kinematic parameters are associated with higher amplitude of flagellar beating and lower progressivity providing them greater vigour and force. Our results showed that estradiol affected VLC or ALH motility parameters depending on mouse strains, stressing the importance of considering strain-base sperm-specific motility differences. In C57BL/6NVel mice, ALH increased at 20 µg/L. In BALB/c, the parameter did not differ from the control, but there was a negative effect of the same concentration on VCL. This result agrees with previously reported sperm motility differences in these mice strains [35]. CASA algorithms calculated ALH based on the specific relationships of VCL and VAP [49]. Thus, our findings are supportive of the analysis of sperm capacitation by TyrP results, (Figure 3, Figure A1, Appendix B in Supplementary Materials) which showed estradiol had a stimulatory effect on the hyperactivation (ALH) of spermatozoa. Having validated experimental systems and relevant biological data regarding the effect of estradiol on sperm capacitation, motility, and AR, we focused on quantification of sperm-estradiol binding during capacitation by HPLC-MS/MS, and analysing sperm-estradiol interactive binding kinetics.

Combining both experimental and theoretical data, we therefore propose a novel estradiol binding pattern. The schematic and simplified interpretation of the kinetic analysis results applied to data obtained from estradiol action in sperm during capacitation is summarized in Figure 8.
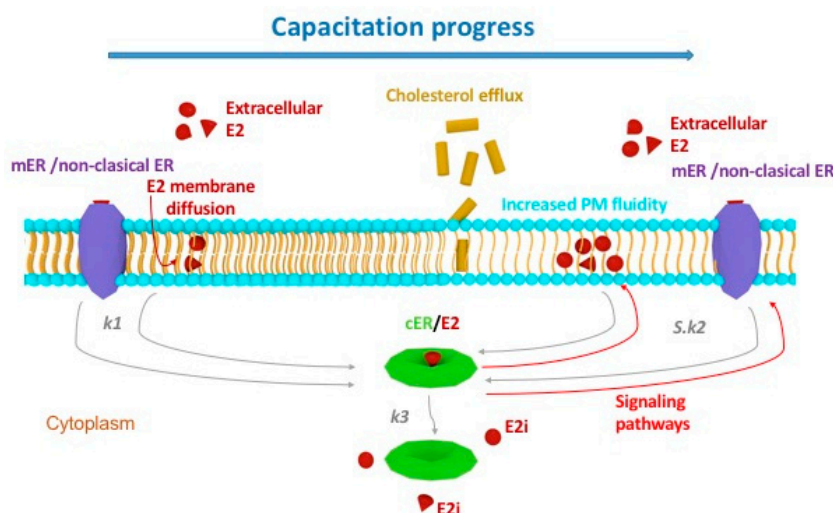
Figure 8. Schematic interpretation of kinetic analysis results applied on estradiol sperm action using the symbols from kinetic equations. The model depicts capacitating progress in time (blue arrow), which is represented by plasma membrane (PM) reorganization and increasing fluidity. During this process, the PM becomes more receiving for extracellular estradiol E2, which is passing via diffusion after its initial adsorption onto specific PM adsorbents, such as mERs and/or non-classical ER. Kinetic analysis of biological data suggests the formation of an adduct cER/E2 in the cytoplasm with the rate constant k_1 (grey arrows), which, when formed, serves as an autocatalytic agent, signalling an increase in PM fluidity directed by $S \cdot k_2$ (red arrows). This signalling event is accompanied by the complex cER/E2 disintegration characterized by the rate constant k_3 (grey arrow) and a release of estradiol $E2_i$ remaining in the cytoplasm. The cERs remain internalized within the cytoplasm; however, they lose their receptivity and remain dormant.

Capacitating sperm undergo several changes including plasma membrane reorganization, which changes its fluidity and improves reception of the extracellular estradiol E2, which passes via diffusion after its initial adsorption (controlled by Langmuir isotherm) onto specific PM adsorbents. These could be represented by mERs and/or non-classical ER. We would like to deliver a hypothesis for this mechanism, suggesting the formation of an adduct in the cytoplasm with the rate constant k_1, which, when formed, serves as an autocatalytic agent, signalling an increase in PM fluidity directed by $S \cdot k_2$, where S is a degree of activity. This signalling event is accompanied by the complex cER/E2 disintegration characterized by the rate constant k_3 and a release of estradiol remaining in the cytoplasm ($E2_i$). The cERs remain internalized within the cytoplasm; however, they lose their receptivity and remain dormant (Appendix A in Supplementary Materials).

One of the criteria for the reliability of kinetic equations is the independence of the rate constants on the concentration conditions. The determined values of the optimized overall constants K_2 and K_3 fulfil these conditions by well over two orders of magnitude. The correctness of the used model was further confirmed by the positions and the shapes of the minima on the $B(t)$ curves, which agreed with the experimental values. The areas around the minima are sensitive to the rate constant values. Hewitt et al. [24] described two processes of estradiol passing through the plasma membrane, one of which is slow and the other is rapid. In our model, the slow process with the rate constant k_1 occurs simultaneously with the rapid (autocatalytic) process, with the rate constant k_2 multiplied by S.

4. Materials and Methods

4.1. Chemicals, Reagents, and Animals

Acetonitrile (ACN) Chromasolv LC/MS and deuterated β-estradiol-16,16,17-d$_3$ (estradiol-d$_3$) (purity 98%) were purchased from Sigma-Aldrich (Chromasolv, Schnelldorf, Germany). Ethanol (96%) was obtained from Lach-Ner (Neratovice, Czech Republic). Paraffin oil was delivered by Carl

Roth (Karlsruhe, Germany). Formic acid (HCOOH) (purity 98–100%) and 17β-estradiol (estradiol) (purity 98%) were provided by Merck (Gernsheim, Germany). Commercial M2 culture media for in vitro sperm capacitation and fertilization (M7167, Sigma-Aldrich, Prague, Czech Republic) contained: HEPES (4-(2-hydroxyethyl)piperazine-1-ethanesulfonic acid), calcium chloride, magnesium sulfate, potassium chloride, potassium phosphate, sodium bicarbonate, sodium chloride, bovine serum albumin, D-glucose, pyruvic acid, and D,L-lactic acid, without penicillin and streptomycin. An experimental M2 medium, but without BSA, was prepared in the Media Preparation and Washing Units, BIOCEV (Vestec, Czech Republic) and used for simulating non-capacitating conditions [1,3]. Deionized water (Milli-Q water purification system Millipore, Billerica, MA, USA) was used in all experiments.

Two laboratory inbreed mouse strains (BALB/c and C57BL/6Nvel) were used for comparative experiments. Mice were purchased from Velaz (Prague, Czech Republic) and maintained and housed at the animal facilities of the Faculty of Science, Charles University (Prague, Czech Republic). All the animal procedures and all the experimental protocols were approved by Local Ethics Committee and carried out in strict accordance with the Animal Scientific Procedure, Art 2010, and subjected to review by this Local Ethics Committee of the Faculty of Science, Charles University, Czech Republic (accreditation no. 247732008-10001).

4.2. Instrumentation and Chromatographic Conditions

The HPLC equipment (Agilent Technologies, Waldbronn, Germany) including a 1290 Infinity Series LC (a quaternary pump, a degasser, a thermostatic auto sampler with a 20 μL sample loop and a column oven). Triple Quad LC/MS 6490 tandem mass spectrometer (Agilent Technologies, Waldbronn, Germany) with an electrospray ionization interface (ESI) was used for the detection. Signals were processed and data were handled with the Mass Hunter Workstation Software (Agilent Technologies, Waldbronn, Germany).

The MS-MS measurements were performed in the multiple reaction monitoring (MRM) mode using ESI ionization in positive mode (ESI (+)). Nitrogen was used as the collision nebulizing and desolvation gas. The optimized ESI (+) conditions in MRM mode for estradiol were as follows: capillary voltage, 5500 V; nebulizer pressure, 60 psi; gas temperature, 350 °C; and nitrogen flow rate 10 L/min. The m/z 255.5 to 158.9 transition (fragmentor voltage: 120 V, collision energy: 14 V) was monitored for estradiol, and the m/z 258.5 to 158.9 transition (fragmentor voltage: 120 V, collision energy: 14 V) was monitored for deuterated estradiol (estradiol-d3).

Separation was performed on a Kinetex EVO C18 column (100 × 3.0 mm i.d., particle size 2.6 μm) from Phenomenex (Torrance, CA, USA). The optimization procedure was carried out to efficiently separate of estradiol in M2 medium [50,51]. Isocratic elution at a flow rate of 0.3 mL/min with the binary solvent system, consisting of 0.1% HCOOH in H_2O and 0.1% HCOOH in 100% ACN, 50/50 (v/v), was selected. The column temperature was held at 21 ± 0.5 °C. The sample injection was 7.5 μL. The retention time of estradiol was 3.1 min. The complex M2 medium contained inorganic and organic components, and BSA (4.0 g/L) can especially cause difficulties during the separation and detection process. The eluate was discharged from 0 to 2.5 min and passed into the MS detector for 2.5 to 4.0 min.

The stock solution of estradiol at 200 mg/L was prepared by dissolving an appropriate amount of estradiol standard in ethanol. The stock solutions at concentration of 20, 2, and 0.2 mg/L were obtained by serial dilutions with ethanol and were stored in the dark at 5 °C. Working solutions to obtain the standard points of the calibration curve were prepared by diluting the appropriate ethanolic stock solutions with capacitating M2 medium to attain the following concentrations: 1, 5, 10, 15, 20, 25, 50, 75, 100, 125, 150, 175, 200, and 225 μg/L. The internal standard (estradiol-d$_3$) working solution was prepared fresh daily in ethanol at a concentration of 250 μg/L. We added 100 μL of this solution to each calibration standard solution to attain the final concentration of 25 μg/L.

Under optimized separation and detection conditions, the calibration curve for estradiol was measured in the concentration range of 1–225 μg/L and the analyte was tested within a linearity range

from limit of quantitation (LOQ) to 225 μg/L. Each measurement of the peak area (peak height) was performed in 5 replicates and the results of the linear regression for the peak area ratio of the analyte to the internal standard versus concentration are listed in Table A3, Appendix B in Supplementary Materials. A satisfactory fit between the experimental points and linear calibration curve was observed. The peak height-concentration dependence was treated by linear regression to determine the limit of detection (LOD) and LOQ, as $3\times$ and $10\times$ noise levels, respectively. The values obtained for LOD and LOQ are presented in Table A3, Appendix B in Supplementary Materials.

4.3. Capacitation of Mouse Sperm In Vitro and Sample Preparation for HPLC-MS/MS Analysis

For the in vitro realization of capacitation, 35- mm Petri dishes obtained from Corning (Corning, NY, USA) were used. An Olympus CX 21 light inverted microscope and Olympus epifluorescent microscope were supplied by Olympus (Prague, Czech Republic). The NB-203 incubator was purchased from N-BIOTEK (Bucheon, Korea). For in vitro cultivation of sperm, incubator Telstar Bio-IIA and laminar box-BioTek from N-BIOTEK (Bucheon, Korea) were used.

The physiological estradiol concentrations relevant to the reproductive system are known in rats, mice, and humans. The concentrations vary from 250 pg/mL in the rete testis fluid in rats [44,52] to 1 ng/mL in the spermatic vein of men [53], and fluctuates in plasma during estrous between 145–2100 pg/mL in rat and mouse [45] and 90–400 pg/mL in woman [54]. In the ovarian fluid, the concentration is at least two-fold higher than in plasma [44,52]. Due to this wide concentration range, the in vitro system, and the detection limit of HPLC/MS-MS, we used the working experimental estradiol solutions with dilutions of 2, 20 and 200 μg/L. These concentrations were prepared by diluting the ethanolic stock solution of estradiol (200, 20 or 2 mg/L) with capacitating M2 medium (Sigma-Aldrich, Prague, Czech Republic) or non-capacitating medium without BSA (Media Preparation and Washing Units, BIOCEV, Vestec, Czech Republic) to attain the required experimental concentration according to the following scheme: 1 μL of appropriate ethanolic solution was diluted into 1 mL of capacitating M2 or non-capacitating medium to minimize the amount of ethanol in biological sample. Then, 100 μL of this solution was placed into each of the Petri dishes and covered with 1 mL paraffin oil. All procedures were performed in a sterile laminar box. Prepared Petri dishes were then placed for 60 min to incubate at 37 °C in 5% CO_2 in air.

The biological sample was prepared in three parallel sets and each set represented sperm collecting from one individual. Spermatozoa, which were recovered from the distal region of the *cauda epididymidis*, were placed in capacitating M2 or non-capacitating medium and left in an incubator for 10 min at 37 °C under 5% CO_2 to relax sperm. After that, the concentration of stock sperm in the medium was adjusted to 5×10^6 sperm/mL. The motility and viability of the sperm population was checked throughout the experiment using a light inverted microscope with a thermostatically controlled stage at 37 °C. It remained unchanged during experimental time and conditions when compared with the stock solution.

There were four groups labelled as follows: (1) M (control, sperm in capacitating medium), (2) M + estradiol (capacitating medium with addition of estradiol: 200, 20, or 2 μg/L), (3) M without BSA (non-capacitating medium), and (4) M without BSA with estradiol (non-capacitating medium with addition of estradiol: 200 μg/L). Samples were prepared in Petri dishes according to the following scheme: after 60 min incubation of 100 μL of 200, 20, or 2 μg/L solution of estradiol in media, 5 μL of sperm stock solution was added. Each time, 6 Petri dishes were used, each one containing 105 μL of sample volume covered with 1 mL paraffin oil. Control samples, using only capacitating M2 or non-capacitating medium without the addition of estradiol, were run in parallel in each experiment. Spermatozoa were incubated (37 °C, 5% CO_2) for up to 3 h. At half hour intervals (0, 30, 60, 90, 120, 150, and 180 min after adding sperm) samples were collected. The sample solutions from all Petri dishes (for a given time) were placed into one micro tube to centrifugate for 10 min at 12,000 rpm to remove the spermatozoa. After centrifugation, 450 μL of the supernatant was placed into a vial for HPLC-MS/MS analysis. To avoid potential systematic errors during sample preparation (partial evaporation of

samples during incubation, differences in collection of supernatant after centrifugation, etc.), reference samples (blanks) were prepared collaterally with the samples described above, but no spermatozoa were added into the incubated estradiol solution. To check the correctness of HPLC-MS/MS analysis, 50 μL of internal standard working solution at a concentration of 250 μg/L was added into each sample before the measurement. Each sample was measured in 5 replicates and the mean value was calculated.

The matrix effect was measured for all tested estradiol concentrations (2, 20, and 200 μg/L) by comparing the peak response of (1) the supernatant prepared by addition of sperm in the medium and after centrifugation spiked with estradiol and with (2) the sample prepared by addition of estradiol directly into the medium and no matrix effect was observed.

4.4. SDS-PAGE with Immunoblotting

SDS (Sodium dodecyl sulfate) electrophoresis and immunoblotting were used for the TyrP assessment, carried out using protocols based on standard methods [55,56]. Suspension of non-capacitated sperm from a sperm stock released from the cauda epididymis was used. Sperm samples were collected at 0, 60, and 90 min of capacitation in vitro, diluted with PBS, and a final concentration of 5×10^6 sperm/mL was ascertained using a Bürker chamber (Sigma-Aldrich, Prague, Czech Republic). Sperm pellets were re-suspended in an equal volume of SDS-PAGE (sodium dodecylsulphate-polyacrylamide gel-electrophoresis) reduced sample buffer and heated at 97 °C for 3 min. Samples containing protein equivalent to 5×10^6 capacitated sperm per mL were run on a 5% stacking and 10% running SDS polyacrylamide gel using Precision Plus Protein™ Dual Color Standards (Bio-Rad, München, Germany) as molecular weight markers. After transferring protein onto a nitrocellulose membrane, nonspecific sites were blocked with PBS blocking solution (5% skimmed milk and 0.05% Tween 20). Proteins phosphorylated on tyrosine residues were identified by the primary MAB (monoclonal antibody) anti-phosphotyrosine P-Tyr-01 (Exbio, Vestec, Czech Republic) diluted 1:300, followed by a peroxidase goat anti-mouse IgG (Immunoglobulin G) secondary antibody (Sigma-Aldrich, Prague, Czech Republic) diluted 1:5000. β tubulin was detected by anti-β tubulin primary antibody ab15568 (Abcam, Cambridge, MA, USA), diluted 1:200, followed by peroxidase goat anti-rabbit IgG secondary antibody 1706515 (Bio-Rad, München, Germany) diluted 1:3000. Protein staining was visualised by chemiluminescence Super Signal West Dura (Thermo Fischer Scientific, Prague, Czech Republic). These experiments were performed four times with similar results. Representative results are shown.

4.5. Statistical Analysis

Experimental data were analyzed using STATISTICA 6.0 (Statsoft, Prague, Czech Republic) and GraphPad Prism 5.04 (GraphPad Software Inc., La Jolla, CA, USA). The differences between the control and experimental groups in the number of TyrP positive sperm heads were analyzed by KW-ANOVA (Kruskal–Wallis test), and post-hoc analysis was performed by Dunn's comparisons: * $p < 0.05$, ** $p < 0.01$, *** $p < 0.001$.

We used R (v 3.4.0) [57] to evaluate the general effects of estradiol concentrations on sperm performance in two mouse strains (BALB/c and C57BL/6Nvel). To avoid pseudo replication, analyses were based on mean trait values measured on each male mouse in respective time and estradiol concentration, rather than on performance of each sperm cell. All three measures of sperm velocity—the strait velocity (VSL), curvilinear velocity (VCL), and the average path velocity (VAP)—were strongly correlated with each other (Pearson product-moment correlation coefficients of 0.97 in all comparisons). As the medium did not contain any component to guide the spermatozoa in one direction, we used curvilinear velocity (VCL) rather than the others measures as our measurement of sperm swimming speed [58,59]. There was only a moderate association between the lateral head displacement (ALH) and three measures of sperm velocity (Pearson product-moment correlation coefficients ranged between 0.39 and 0.58). Therefore, VCL and lateral head displacement (ALH) were analyzed separately. We used the lmer() function in the lme4 package [59] for fitting linear mixed effect model with either

sperm motility (VCL) or the amplitude of ALH as the dependent variable and estrogen concentration (categorical variable with four levels: control, 2, 20, and 200 µg/L), strain identity, and their two-way interaction as fixed effects. To control for repeated observation within male mice over time, male identity was included as random intercept and time of measurement (0, 30, 60, and 120 min) as random slope. To obtain *p*-values, we performed likelihood ratio tests comparing models with and without a specific fixed effect.

5. Conclusions

Based on presented data, estradiol has a stimulatory effect on protein tyrosine phosphorylation, lateral head displacement, and spontaneous acrosome reaction during in vitro mouse sperm capacitation. The level of estradiol available for mouse spermatozoa during capacitation in vitro was quantified by HPLC-MS/MS and data were subjected to kinetic analysis. The proposed kinetic model explains the crosstalk between estradiol and both receptor and non-receptor pathways, suggesting an autocatalytic signalling pattern as a novel mechanism utilized by sperm prior to fertilization. There is a potential in this new analytical-biological approach for understanding the physiological mechanism of steroid hormones, including estradiol, not only in reproductive biology, but also in somatic cell signalling events, both physiological and pathological, targeting mainly cancer cell biology research.

References

1. Yanagimachi, R. Mammalian fertilization. In *The Physiology of Reproduction*; Knobil, E., Neill, J.D., Eds.; Raven Press: New York, NY, USA, 1994; pp. 189–317.

2. Naz, R.K.; Rajesh, P.B. Role of tyrosine phosphorylation in sperm capacitation/acrosome reaction. *Reprod. Biol. Endocrinol.* **2004**, *2*, 75–87. [CrossRef] [PubMed]

3. Visconti, P.E.; Bailey, J.L.; Moore, G.D.; Pan, D.; Olds-Clarke, P.; Kopf, G.S. Capacitation of mouse spermatozoa. I. Correlation between the capacitation state and protein tyrosine phosphorylation. *Development* **1995**, *121*, 1129–1137. [PubMed]

4. Wang, J.; Qi, L.; Huang, S.; Zhou, T.; Guo, Y.; Wang, G.; Guo, X.; Zhou, Z.; Sha, J. Quantitative Phosphoproteomics Analysis Reveals a Key Role of IGF1R Tyrosine Kinase in Human Sperm Capacitation. *Mol. Cell. Proteomics* **2015**, *14*, 1104–1112. [CrossRef] [PubMed]

5. Alvau, A.; Battistone, M.A.; Gervasi, M.G.; Navarrete, F.A.; Xu, X.; Sánchez-Cárdenas, C.; De la Vega-Beltran, J.L.; Da Ros, V.G.; Greer, P.A.; Darszon, A.; et al. The tyrosine kinase FER is responsible for the capacitation-associated increase in tyrosine phosphorylation in murine sperm. *Development* **2016**, *143*, 2325–2333. [CrossRef] [PubMed]

6. Itach, S.B.; Finkelstein, M.; Etkovitz, N.; Breitbart, H. Hyper-activated motility in sperm capacitation is mediated by phospholipase D-dependent actin polymerization. *Dev. Biol.* **2012**, *362*, 154–161. [CrossRef] [PubMed]

7. Suarez, S.S.; Pacey, A.A. Sperm transport in the female reproductive tract. *Hum. Reprod. Update* **2006**, *12*, 23–37. [CrossRef] [PubMed]

8. Peknicová, J.; Kyselová, V.; Boubelík, M.; Buckiová, D. Effect of an endocrine disruptor on mammalian fertility. Application of monoclonal antibodies against sperm proteins as markers for testing sperm damage. *Am. J. Reprod. Immunol.* **2002**, *47*, 311–318. [CrossRef]

9. Baldi, E.; Luconi, M.; Muratori, M.; Marchiani, S.; Tamburrino, L.; Forti, G. Nongenomic activation of spermatozoa by steroid hormones: Facts and fictions. *Mol. Cell. Endocrinol.* **2009**, *308*, 39–46. [CrossRef]

10. Ded, L.; Dostalova, P.; Dorosh, A.; Dvorakova-Hortova, K.; Peknicova, J. Effect of estrogens on boar sperm capacitation in vitro. *Reprod. Biol. Endocrinol.* **2010**, *8*, 87. [CrossRef]

11. Sebkova, N.; Cerna, M.; Ded, L.; Peknicova, J.; Dvorakova-Hortova, K. The slower the better: How sperm capacitation and acrosome reaction is modified in the presence of estrogens. *Reproduction* **2012**, *143*, 297–307. [CrossRef]

12. Ded, L.; Sebkova, N.; Cerna, M.; Elzeinova, F.; Dostalova, P.; Peknicova, J.; Dvorakova-Hortova, K. In vivo exposure to 17β-estradiol triggers premature sperm capacitation in cauda epididymis. *Reproduction* **2013**, *145*, 255–263. [CrossRef] [PubMed]

13. Luconi, M.; Muratori, M.; Forti, G.; Baldi, E. Identification and characterization of a novel functional estrogen receptor on human sperm membrane that interferes with progesterone effects. *J. Clin. Endocrinol. Metabol.* **1999**, *84*, 1670–1678. [CrossRef] [PubMed]

14. Noguchi, T.; Fujinoki, M.; Kitazawa, M.; Inaba, N. Regulation of hyperactivation of hamster spermatozoa by progesterone. *Reprod. Med. Biol.* **2008**, *7*, 63–74. [CrossRef] [PubMed]

15. Fujinoki, M. Suppression of progesterone-enhanced hyperactivation in hamster spermatozoa by estrogen. *Reproduction* **2010**, *140*, 453–464. [CrossRef] [PubMed]

16. Fujinoki, M. Regulation and disruption of hamster sperm hyperactivation by progesterone, 17β-estradiol and diethylstilbestrol. *Reprod. Med. Biol.* **2014**, *13*, 143–152. [CrossRef] [PubMed]

17. Aquila, S.; De Amicis, F. Steroid receptors and their ligands: Effects on male gamete functions. *Exp. Cell Res.* **2014**, *328*, 303–313. [CrossRef] [PubMed]

18. Dostalova, P.; Zatecka, E.; Dvorakova-Hortova, K. Of Oestrogens and Sperm: A Review of the Roles of Oestrogens and Oestrogen Receptors in Male Reproduction. *Int. J. Mol. Sci.* **2017**, *18*, 904. [CrossRef]

19. Marino, M.; Acconcia, F.; Bresciani, F.; Weisz, A.; Trentalance, A. Distinct nongenomic signal transduction pathways controlled by 17beta-estradiol regulate DNA synthesis and cyclin D(1) gene transcription in HepG2 cells. *Mol. Biol. Cell* **2002**, *13*, 3720–3729. [CrossRef]

20. Acconcia, F.; Ascenzi, P.; Bocedi, A.; Spisni, E.; Tomasi, V.; Trentalance, A.; Visca, P.; Marino, M. Palmitoylation-dependent estrogen receptor alpha membrane localization: Regulation by 17beta-estradiol. *Mol. Biol. Cell* **2005**, *16*, 231–237. [CrossRef]

21. Ahola, T.M.; Manninen, T.; Alkio, N.; Ylikomi, T. G protein-coupled receptor 30 is critical for a progestin-induced growth inhibition in MCF-7 breast cancer cells. *Endocrinology* **2002**, *143*, 3376–3384. [CrossRef]

22. Thomas, P.; Pang, Y.; Filardo, E.J.; Dong, J. Identity of an estrogen membrane receptor coupled to a G protein in human breast cancer cells. *Endocrinology* **2005**, *146*, 624–632. [CrossRef] [PubMed]

23. Vivacqua, A.; Bonofiglio, D.; Recchia, A.G.; Musti, A.M.; Picard, D.; Andò, S.; Maggiolini, M. The G protein-coupled receptor GPR30 mediates the proliferative effects induced by 17beta-estradiol and hydroxytamoxifen in endometrial cancer cells. *Mol. Endocrinol.* **2006**, *20*, 631–646. [CrossRef] [PubMed]

24. Hewitt, S.C.; Deroo, B.J.; Korach, K.S. Signal transduction. A new mediator for an old hormone? *Science* **2005**, *307*, 1572–1573. [CrossRef] [PubMed]

25. Manavathi, B.; Kumar, R. Steering estrogen signals from the plasma membrane to the nucleus: Two sides of the coin. *J. Cell. Physiol.* **2006**, *207*, 594–604. [CrossRef] [PubMed]

26. Marino, M.; Galluzzo, P.; Ascenzi, P. Estrogen signaling multiple pathways to impact gene transcription. *Curr. Genomics* **2006**, *7*, 497–508. [CrossRef] [PubMed]

27. Klinge, C.M. Estrogen receptor interaction with estrogen response elements. *Nucleic Acids Res.* **2001**, *29*, 2905–2919. [CrossRef] [PubMed]

28. Li, C.; Briggs, M.R.; Ahlborn, T.E.; Kraemer, F.B.; Liu, J. Requirement of Sp1 and estrogen receptor alpha interaction in 17beta-estradiol-mediated transcriptional activation of the low density lipoprotein receptor gene expression. *Endocrinology* **2001**, *142*, 1546–1553. [CrossRef] [PubMed]

29. Safe, S.H.; Pallaroni, L.; Yoon, K.; Gaido, K.; Ross, S.; Saville, B.; McDonnell, D. Toxicology of environmental estrogens. *Reprod. Fertil. Dev.* **2001**, *13*, 307–315. [CrossRef]

30. Stossi, F.; Likhite, V.S.; Katzenellenbogen, J.A.; Katzenellenbogen, B.S. Estrogen-occupied estrogen receptor represses cyclin G2 gene expression and recruits a repressor complex at the cyclin G2 promoter. *J. Biol. Chem.* **2006**, *281*, 16272–16278. [CrossRef] [PubMed]

31. Glass, C.K.; Rosenfeld, M.G. The coregulator exchange in transcriptional functions of nuclear receptors. *Genes Dev.* **2000**, *14*, 121–141. [CrossRef]

32. McKenna, N.J.; O'Malley, B.W. Combinatorial control of gene expression by nuclear receptors and coregulators. *Cell* **2002**, *108*, 465–474. [CrossRef]

33. Sztein, J.M.; Farley, J.S.; Mobraaten, L.E. In vitro fertilization with cryopreserved inbred mouse sperm. *Biol. Reprod.* **2000**, *63*, 1774–1780. [CrossRef] [PubMed]

34. Liu, L.; Nutter, L.M.; Law, N.; McKerlie, C. Sperm freezing and in vitro fertilization in three substrains of C57BL/6 mice. *J. Am. Assoc. Lab. Anim. Sci.* **2009**, *48*, 39–43. [PubMed]

35. Goodson, S.G.; Zhang, Z.; Tsuruta, J.K.; Wang, W.; O'Brien, D.A. Classification of mouse sperm motility patterns using an automated multiclass support vector machines model. *Biol. Reprod.* **2011**, *84*, 1207–1215. [CrossRef] [PubMed]

36. Bosakova, Z.; Tockstein, A.; Adamusova, H.; Coufal, P.; Sebkova, N.; Dvorakova-Hortova, K. Kinetic analysis of decreased sperm fertilizing ability by fluorides and fluoroaluminates: A tool for analyzing the effect of environmental substances on biological events. *Eur. Biophys. J.* **2016**, *45*, 71–79. [CrossRef] [PubMed]

37. Dvořáková-Hortová, K.; Šandera, M.; Jursová, M.; Vašinová, J.; Pěknicová, J. The influence of fluorides on mouse sperm capacitation. *Anim. Reprod. Sci.* **2008**, *108*, 157–170. [CrossRef] [PubMed]

38. Davis, B.K.; Byrne, R.; Hungund, B. Studies on the mechanism of capacitation. II. Evidence for lipid transfer between plasma membrane of rat sperm and serum albu min during capacitation in vitro. *Biochim. Biophys. Acta* **1979**, *558*, 257–266. [CrossRef]

39. Dow, M.P.D.; Bavister, B.D. Direct contact is required between serum albu min and hamster spermatozoa for capacitation in vitro. *Gamete Res.* **1989**, *23*, 171–180. [CrossRef]

40. Romeu, A.M.; Martino, E.E.; Stoppani, A.O.M. Structural requirements for the action of steroids as quenchers of albu min fluorescence. *Biochim. Biophys. Acta* **1975**, *409*, 376–386. [CrossRef]

41. Stewart-Savage, J. Effect of bovine serum albu min concentration and source on sperm capacitation in the golden hamster. *Biol. Reprod.* **1993**, *49*, 74–81. [CrossRef]

42. Asquith, K.L.; Baleato, R.M.; McLaughlin, E.A.; Nixon, B.; Aitken, R.J. Tyrosine phosphorylation activates surface chaperones facilitating sperm–zona recognition. *J. Cell. Sci.* **2004**, *117*, 3645–3657. [CrossRef] [PubMed]

43. Nishimura, I.; Ui-Tei, K.; Saigo, K.; Ishii, H.; Sakuma, Y.; Kato, M. 17-Estradiol at physiological concentrations augments Ca2+-activated K+ currents via estrogen receptor in the gonadotropin-releasing hormone neuronal cell line GT1-7. *Endocrinology* **2008**, *149*, 774–782. [CrossRef] [PubMed]

44. Hess, R.A.; Bunick, D.; Bahr, J.M. Sperm, a source of estrogen. *Environ. Health Perspect.* **1995**, *103*, 59–62. [CrossRef] [PubMed]

45. Shaikh, A.A. Estrone and estradiol levels in the ovarian venous blood from rats during the estrous cycle and pregnancy. *Biol. Reprod.* **1971**, *5*, 297–307. [CrossRef] [PubMed]

46. Tarlatzis, B.C.; Pazaitou, K.; Bili, H.; Bontis, J.; Papadimas, J.; Lagos, S.; Spanos, E.; Mantalenakis, S. Growth hormone, oestradiol, progesterone andtestosterone concentrations in follicular fluid after ovarian stimulation with various regimes for assisted reproduction. *Hum. Reprod.* **1993**, *8*, 1612–1616. [CrossRef] [PubMed]

47. Jin, M.; Fujiwara, E.; Kakiuchi, Y.; Okabe, M.; Satouh, Y.; Baba, S.A.; Chiba, K.; Hirohashi, N. Most fertilizing mouse spermatozoa begin their acrosome reaction before contact with the zona pellucida during in vitrofertilization. *Proc. Natl. Acad. Sci. USA* **2011**, *108*, 4892–4896. [CrossRef] [PubMed]

48. Inoue, N.; Satouh, Y.; Ikawa, M.; Okabe, M.; Yanagimachi, R. Acrosome reacted mouse spermatozoa recovered from the perivitelline space can fertilize other eggs. *Proc. Natl. Acad. Sci. USA* **2001**, *108*, 20008–20011. [CrossRef] [PubMed]

49. Mortimer, S.T.; van der Horst, G.; Motimer, D. The future of computer-aided sperm analysis. *Asian J. Androl.* **2015**, *17*, 545–553. [CrossRef]

50. Kozlík, P.; Bosáková, Z.; Tesařová, E.; Coufal, P.; Čabala, R. Development of a solid-phase extraction with capillary liquid chromatography tandem mass spectrometry for analysis of estrogens in environmental water samples. *J. Chromatogr. A* **2011**, *1218*, 2127–2132. [CrossRef]

51. Dvorakova-Hortova, K.; Honetschlägerová, M.; Tesařová, E.; Vašinová, J.; Frolíková, M.; Bosáková, Z. Residual concentration of estriol during mouse sperm capacitation in vitro determined by HPLC method. *Folia Zool.* **2009**, *58*, 75–81.

52. Free, M.J.; Jaffe, R.A. Collection of rete testis fluid from rats without previous efferent duct ligation. *Biol. Reprod.* **1979**, *20*, 269–278. [CrossRef] [PubMed]

53. Kelch, R.P.; Jenner, M.R.; Weinstein, R.; Kaplan, S.L.; Grumbach, M.M. Estradiol and testosterone secretion by human, simian, and canine testes, in males with hypogonadism and in male pseudohermaphrodites with the feminizing testes syndrome. *J. Clin. Investig.* **1972**, *51*, 824–830. [CrossRef] [PubMed]

54. Abraham, G.E.; Odell, W.D.; Swerdloff, R.S.; Hopper, K. Simultaneous radioimmunoassay of plasma FSH, LH, progesterone, 17-hydroxyprogesterone, and estradiol-17 during the menstrual cycle. *J. Clin. Endocrinol. Metabl.* **1972**, *34*, 312–318. [CrossRef]

55. Laemmli, U.K. Cleavage of structural proteins during assembly of the head of bacteriophage T4. *Nature* **1970**, *227*, 680–685. [CrossRef] [PubMed]

56. Zigo, M.; Jonakova, V.; Manaskova-Postlerova, P. Electrophoretic and zymographic characterization of proteins isolated by various extraction methods from ejaculated and capacitated boar sperms. *Electrophoresis* **2011**, *32*, 1309–1318. [CrossRef] [PubMed]

57. R Core Team. *R: A Language and Environment for Statistical Computing*; R Foundation for Statistical Computing: Vienna, Austria, 2017.

58. Opatova, P.; Ihle, M.; Albrechtova, J.; Tomasek, O.; Kempenaers, B.; Forstmeier, W. Inbreeding depression of sperm traits in the zebra finch Taeniopygia guttata. *Ecol. Evol.* **2016**, *6*, 295–304. [CrossRef] [PubMed]

59. Bates, D.; Mächler, M.; Bolker, B.; Walker, S. Fitting linear mixed-effects models using lme4. *J. Stat. Softw.* **2015**, *67*, 1–48. [CrossRef]

New insight into sperm capacitation: A novel mechanism of 17β-estradiol signaling

Appendix A

Material and Methods

Kinetic analysis

In the search for various kinetic models it was found that, for the agreement between the curves obtained by fitting through the experimental points and the theoretical calculated curves, it is necessary to assume that the first step is adsorption of estradiol onto the surface of the sperm controlled by Langmuir isotherm. Other models (without adsorption) lead to completely different results.

The following model in which the symbols of the species also correspond to their molar concentrations was used for the autocatalytic process. The Langmuir adsorption of estradiol onto the surface of sperm PM first occurs with a starting estradiol concentration ($E2_0$), and the surface of PM at these sites (number n_a) becomes more accessible. It holds for n_a that: $n_a = \frac{zw(E2_0)}{1+w(E2_0)}$ where z is the maximum number of adsorption sites ((mER) or membrane non-estrogen receptors) and w is the adsorption coefficient. Well below the saturation point ($1 > w\,(E2_0)$) it holds that $n_a = z\,w\,(E2_0)$. At sites n_a the externally present estradiol (concentration of extracellular estradiol at the time > 0, ($E2$)) reacts with the sperm membrane receptors leading to increased permeability of PM, through which estradiol molecules are transported within the cytoplasm to (cER) and forming the adduct (($E2$)/(cER)). This is connected with a further increase in the PM permeability. The primary penetration of PM corresponds to the following kinetic product, where k_1 is the rate constant corresponding to the formation of aduct:

$k_1\,n_a\,(E2)\,(cER)$ (1a)

The gradual growth of adducts (($E2$)/(cER)) in the cytoplasm leads to ever increasing permeability of PM (signalling). Activity Γ increases and is proportional to the consumed estradiol $\Gamma = k\,((E2_0) - (E2))$ so that, at the end of the reaction, $\Gamma_\infty = k\,(E2_0)$, the degree of activity S can be defined as: $S = \frac{\Gamma}{\Gamma_\infty} = \frac{(E2_0)-(E2)}{(E2_0)}$

The formation of the adduct (($E2$)/(cER)) is thus enriched by the autocatalytic reaction, with the corresponding kinetic product:

$k_2\,(E2)\,(cER)\,S$ (1b)

where k_2 is the rate constant corresponding to the elevated degree of permeability of PM through the formation of adduct (($E2$)/(cER)) in the cytoplasm. The formed adduct (($E2$)/(cER)) is not stable and decomposes with the formation of internal estradiol (i.e.

inside the cytoplasm, $(E2_i)$) and this kinetic equation corresponds to the kinetic product:

$$k_3\,((E2)/(cER)) \tag{1c}$$

where k_3 is the rate constant corresponding to the decomposition $((E2)/cER))$ of the adduct.

Thus, using Eqs.1a – c, we can write for the overall rates of the individual steps:

$$\frac{-d(E2)}{dt} = k_1 z\, w\,(E2_0)\,(E2)\,(cER) + k_2\, S\,(E2)\,(cER) \tag{2a}$$

$$\frac{-d(cER)}{dt} = k_1 z\, w\,(E2_0)\,(E2)\,(cER) + k_2\, S\,(E2)\,(cER) \tag{2b}$$

$$\frac{d((E2)/(cER))}{dt} = k_1 z\, w\,(E2_0)(E2)\,(cER) + k_2\, S\,(E2)\,(cER) - k_3\,((E2)/(cER)) \tag{2c}$$

$$\frac{d(E2_i)}{dt} = k_3\,((E2)/(cER)) \tag{2d}$$

with the following initial conditions:

$(E2)_{(t=0)} = (E2_0)$, $((E2)/(cER))_{(t=0)} = 0$, $(E2_i)_{(t=0)} = 0$, $(cER)_{(t=0)} = (cER_0)$

It follows from Eqs.2a, b that:

$$\frac{d(E2)}{dt} = \frac{d(cER)}{dt}, \text{ and after integration: } (E2) - (E2_0) = (cER) - (cER_0) \tag{3a}$$

adding Eqs. 2a, c, d yields: $\frac{d(E2)}{dt} + \frac{d((E2)/((cER))}{dt} + \frac{d(E2_i)}{dt} = 0$ and, after integration:

$$(E2) - (E2_0) + ((E2)/(cER)) + (E2_i) = 0 \tag{3b}$$

In the next step we express from Eq.3a: $(cER) = (E2) - (E2_0) + (cER_0)$, substituting into Eqs. 2a, c where simultaneously we write S as $\frac{(E2_0)-(E2)}{(E2_0)}$ and rearrange:

$$\frac{-d(E2)}{dt} = (E2)((E2) - (E2_0) + (cER_0))(k_1 z\, w\,(E2_0) + k_2\left(1 - \frac{(E2)}{(E2_0)}\right)) \tag{4a}$$

$$\frac{d((E2)/(cER))}{dt} = (E2)((E2) - (E2_0) + (cER_0))(k_1 z\, w\,(E2_0) + k_2\left(1 - \frac{(E2)}{(E2_0)}\right)) - k_3((E2)/$$
$$(cER)) \tag{4b}$$

$$\frac{d(E2_i)}{dt} = k_3((E2)/(cER)) \tag{4c}$$

Internal $(E2_i)$ is formed after decomposition $((E2)/(cER))$ and then it follows from Eq.3b that:

$$(E2_i) = (E2_0) - (E2) - ((E2)/(cER)) \tag{4d}$$

In the above-described measuring method, after completion of the reaction by intense centrifugation, the centrifugate contains both internal $(E2_i)$ and extracellular $(E2)$ estradiol and the sperm together with the adduct $((E2)/(cER))$ remain in the sediment. The measured concentration (C) is proportional to the total unbound estradiol content: $k\,((E2) + (E2_i))$ and Eq.4d yields its theoretical value:

$$C = k\big((E2_0) - ((E2)/(cER))\big), \quad C_0 = k\,(E2_0) \tag{5a}$$

In order to simplify the set of Eqs. 4a, b as much as possible, minimize the number of variables and eliminate unknown values of constants z, w and (cER_0), the relative concentrations will now be introduced: $\varepsilon = \frac{(E2)}{(E2_0)}$, $\alpha = \frac{((E2)/(cER))}{(E2_0)}$, the molar ratio $n = \frac{(E2_0)}{(cER_0)}$, dimensionless time $\tau = t\,(cER_0)\,k_1 z\,w\,(E2_{01}) = t\,(cER_0)\,K_1$, (so that $K_1 = k_1 z\,w\,(E2_{01})$) and also constants $K_2 = \frac{k_2}{K_1}$, $K_3 = \frac{k_3}{(cER_0)K_1}$ and fraction $D = \frac{(E2_0')}{(E2_{01})}$, where it is best to take the highest added estradiol concentration for $(E2_{01})$ and $(E2_0')$ is the currently selected initial estradiol concentration, so that $\frac{(E2_0')}{(E2_{01})}$ can assume values of 1, 0.1 or 0.01. Thus, the D values are fixed by dilution.

The $B(t)$ value for the sperm of the BALB/c and C57BL/6Nvel strains of mice can then be expressed as:

$$B(t) = 1 - \frac{((E2)/(cER))}{(E2_0)}, \text{ thus } B(t) = 1 - \alpha \tag{5b}$$

The set of differential Eqs.4a – c then changes to the form:

$$\frac{-d\varepsilon}{d\tau} = \varepsilon\,(n(\varepsilon - 1) + 1)\,(D + K_2(1 - \varepsilon)) \tag{6a}$$

$$\frac{d\alpha}{d\tau} = \varepsilon\,(n(\varepsilon - 1) + 1)\big(D + K_2(1 - \varepsilon)\big) - K_3\alpha \tag{6b}$$

with initial conditions $\varepsilon_{(t=\infty)} = 1$ and $\alpha_{(t=0)} = 0$.

The reaction is theoretically terminated for $n < 1$, when $\varepsilon = 0$, $\alpha = 0$ and thus $B_{t\infty} = 1$. For $n > 1$ the reaction is terminated for $(cER) = 0$, or $n(\varepsilon - 1) + 1 = 0$, so that $\varepsilon_{(t=\infty)} = 1 - \frac{1}{n}$. According to Eq.5b, it also holds for $\alpha = 0$ that $B_{t\infty} = 1$. Thus, all the curves end at limiting value 1. Equations 6a, b are solved by the fourth-order Runge-Kutta method with step of $h = 10^4$. The actual time t is one hundred times greater than the calculated time τ and the results of the calculations are given in Table 2. Values D were determined by diluting the highest employed estradiol concentrations (200μg/L), corresponding to a value of $D = 1$. The molar ratio n was estimated from the shape of curve $B(t)$ for dilution of $D = 1$. The other dilutions are given by a tenth and hundredth

of the original value. Constants K_2 and K_3 were obtained by optimization (searching the minimum of absolute values of the difference between theoretical and experimentally obtained B_t values).

Acrosome reaction

Petri dishes were prepared containing either 100μL of M2 medium under paraffin oil (control) or 100μL of M2 medium containing concentrations of estradiol (200, 20 and 2μg/L) and capacitated for 90min as stated above in Capacitation method. The experimental dishes containing individual estradiol concentrations had the following set up: 1: estradiol alone was present in the M2 medium from the beginning of sperm capacitation (time 0); 2: progesterone (10μM, 3144μg/L) was added to the medium together with estradiol at the beginning of capacitation (time 0); 3: Both estradiol and progesterone were added after 90min of capacitation and sperm were incubated for an additional 90min.

Sperm smears were prepared for every *in vitro* experiment stated above. Sperm were washed twice in PBS, smeared onto glass slides, air dried and fixed with 3.7% formaldehyde in PBS (pH 7.34) at room temperature for 10min, followed by washing in PBS. PNA lectin (Molecular Probes) was added at the concentration of 2.5mM in PBS. After washing, the slides were mounted into Vectashield mounting medium with DAPI (Vector Lab., Burlingame, CA, USA). The samples were examined with an Olympus IX81 fluorescent microscope. The rate of AR was monitored in 200 sperm in six individual experiments for control and each estradiol concentration and experimental groups.

Immunofluorescent detection of sperm heads protein TyrP

Sperm samples were spread on microscope slides. After air-drying, sperm were fixed with 3.7% formaldehyde in PBS (pH 7.34) at room temperature for 10min. Slides were washed with PBS which was followed by immunofluorescent staining. Sperm were blocked with 10% BSA in PBS for 1h and incubated with primary MAB anti-phosphotyrosine P-Tyr-01 (Exbio, Prague, Czech Republic) diluted 1:500 in 1% BSA in PBS over night at 4°C, followed by Alexa Fluor 488 donkey anti-mouse IgG (Molecular Probes, Prague, Czech Republic) secondary antibody 1:1000 in PBS for 1h. Slides were mounted in Vectashield mounting medium with DAPI (Vector Laboratories, Burlingame, CA, USA). Slides were examined with an epifluorescent microscope. For every experiment, we collected sperm data from eight mice. The positive or negative signal was evaluated from a total of 200 spermatozoa on every slide. In each group, at least two samples were analyzed. Data were analyzed statistically.

Analysis of sperm motility

Sperm motility parameters were analysed in experimental groups 1: M (control, sperm in capacitating medium) and 2: M + estradiol (capacitating medium with addition of estradiol - 200, 20 or 2μg/L). Preparation of samples was done in Petri dishes according to the following scheme: after 60min incubation of 100μL of 200, 20 or 2μg/L solution of estradiol in media, sperm stock solution was added to obtain a final concentration of 5x10⁶ sperm/mL. Each time 4 Petri dishes were used, each one

contained $105\mu L$ of sample volume covered with 1mL of paraffin oil. Spermatozoa were incubated (37°C, 5% CO_2) for up to 2h. At intervals (0, 30, 60, 90, 120 min after adding sperm) samples were collected. CASA Hamilton Thorne CEROS (Hamilton Thorne, Inc., USA) was used for sperm motility measurement. The system comprises of a computer, microscope (CX41, Olympus) with negative phase contrast, heating table and a camera (UI-1540-C, Olympus). Sperm tracks were captured in minimally 10 fields at 37°C with a10x negative phase contrast objective (1). Afterwards, recordings were controlled in playback mode to avoid objects, which were not spermatozoa.

Sperm suspensions were gently homogenized before analysis. For each motility measurement $30\mu l$ of sample was loaded into a chamber ($100\mu m$ depth) of pre-warmed Leja Slide (Netherlands). To minimize an effect of flowing liquid, excess was removed from outside by cellulose tissue as recommended by the manufacturer. Recording was performed in the entire area of the chamber, but recorded fields were located out of edges to avoid Segre-Silberberg effect (2). Track and kinematics parameters were recorded for individual spermatozoa. Following kinematic parameters were analysed: curvilinear velocity (VCL, $\mu m/s$), average path velocity (VAP, $\mu m/s$), straight line velocity (VSL, $\mu m/s$) and amplitude of lateral head displacement (ALH, μm).

Reference

1. Albrechtová, J.; Albrecht, T.; Baird, S.J.E.; Macholán, M.; Rudolfsen, G.; Munclinger, P.; Tucker, P.J.; Piálek, J. Sperm-related phenotypes implicated in both maintenance and breakdown of a natural species barrier in the house mouse. *Proc. Roy. Soc.* **2012,** *B 279*, 4803-4810. doi: 10.1098/rspb.2012.1802
2. Douglas-Hamilton, D.H.; Smith, N.G.; Kuster, C.E.; Vermeiden, J.P.W.; Althouse, G.C. Particle Distribution in Low-Volume Capillary-Loaded Chambers. *J Androl* **2005**, *26*, 107-114. doi: 10.1002/j.1939-4640.2005.tb02879.x

Appendix B

Tables and Figures

Table A1. The mean concentrations (C, µg/L) of total unbound estradiol and their standard deviations ($n' = 3$) obtained by HPLC-MS/MS for three tested concentrations (200, 20 and 2 µg/L); the mean values were calculated as the average of the mean values (each sample was measured in 5 replicates) obtained for three parallel sets.

200 µg/L			
Capacitation time (min)	BALB/c	C57BL/6Nvel	Blank
0	196.00 ± 0.80	195.50 ± 0.73	195.70 ± 0.40
30	189.14 ± 0.75	184.53 ± 0.68	196.00 ± 0.60
60	192.67 ± 0.72	186.20 ± 0.30	195.70 ± 0.20
90	193.91 ± 0.86	189.93 ± 0.82	196.00 ± 0.70
120	195.10 ± 0.65	191.50 ± 0.71	196.00 ± 0.50
150	195.41 ± 0.50	192.37 ± 0.77	196.40 ± 0.10
180	195.61 ± 0.70	193.36 ± 0.80	196.10 ± 0.60

20 µg/L			
Capacitation time (min)	BALB/c	C57BL/6Nvel	Blank
0	17.90 ± 0.60	18.10 ± 0.50	18.30 ± 0.20
30	17.28 ± 0.40	17.39 ± 0.20	18.25 ± 0.15
60	16.45 ± 0.10	16.97 ± 0.20	18.40 ± 0.25
90	15.64 ± 0.40	16.36 ± 0.30	18.30 ± 0.10
120	15.86 ± 0.30	16.67 ± 0.30	18.35 ± 0.25
150	16.36 ± 0.40	16.92 ± 0.20	18.20 ± 0.30
180	16.96 ± 0.20	17.30 ± 0.10	18.25 ± 0.29

2 µg/L			
Capacitation time (min)	BALB/c	C57BL/6Nvel	Blank
0	1.60 ± 0.10	1.69 ± 0.06	1.71 ± 0.05
30	1.58 ± 0.05	1.67 ± 0.05	1.70 ± 0.04
60	1.55 ± 0.07	1.64 ± 0.07	1.72 ± 0.04
90	1.50 ± 0.06	1.56 ± 0.06	1.71 ± 0.04
120	1.34 ± 0.09	1.45 ± 0.08	1.69 ± 0.05
150	1.20 ± 0.10	1.38 ± 0.05	1.71 ± 0.04
180	1.24 ± 0.09	1.60 ± 0.07	1.70 ± 0.03

Table A2. Results of linear mixed-effect models involving curvilinear velocity (VCL) or the amplitude of lateral head displacement (ALH) as dependent variables, and estradiol concentration as fixed explanatory variable in two inbred mouse strains. Male identity ($n = 3$ in BALB/c and 4 in C57BL/6N) was included as random intercept, while time of recording (0s, 30s, 60s and 120s) was included as random slope. Treatment contrasts (estradiol concentration = 0) are shown, with control group mean values as intercepts; values for other groups are expressed as differences (and associated standard errors) between the mean of each group and mean of the respective control group.

	BALB/c		C57BL/6N	
Estradiol concentrations	Estimate [SE]	*t*-value	Estimate [SE]	*t*-value
VLC				
control (intercept)	82.88 [3.17]	26.13	107.99 [4.41]	24.47
2μg/L	-12.78 [3.45]	-3.71	-0.14 [2.58]	-0.05
20μg/L	-7.98 [3.45]	-2.35	-2.61 [2.58]	-1.01
200μg/L	-1.52 [3.45]	-0.44	0.08 [2.58]	0.03
ALH				
control (intercept)	12.04 [0.34]	35.95	12.41 [0.20]	61.15
2μg/L	-0.38 [0.47]	-0.78	0.43 [0.25]	1.69
20μg/L	-0.85 [0.47]	-1.79	0.74 [0.25]	2.89
200μg/L	0.08 [0.47]	0.17	0.40 [0.25]	1.55

Table A3. Parameters of the calibration curve (standard deviations in parentheses), limit of detection (LOD) and quantitation (LOQ) for estradiol in M2 capacitating medium, a.u – arbitrary unit.

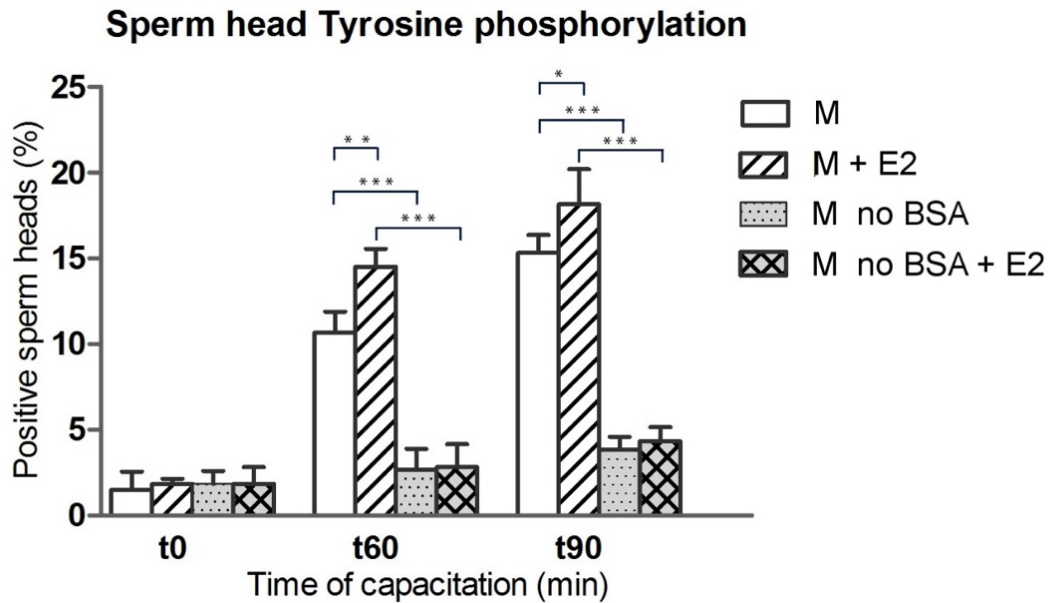| Compound	Slope (L/μg a.u.·s)	Intercept (a.u.·s)	Correlation coefficient	LOD (μg/L)	LOQ (μg/L)
Estradiol	0.0152 (0.0033)	0.0704 (0.0091)	0.9955	0.3	1.1

Figure A1. Sperm head Tyrosine phosphorylation. Number of positive sperm heads for protein TyrP after 0, 60 and 90min of capacitation in presence of estradiol (E2) under capacitating (capacitating M2 medium: M/M+E2) and non-capacitating (BSA absence in the medium: M no BSA/M no MSA+E2) conditions evaluated by immunofluorescent staining. Capacitation progress was measured by anti-TyrP antibody. *P<0.05, **P<0.01, ***P<0.001.

Reference

1. Albrechtová, J.; Albrecht, T.; Baird, S.J.E.; Macholán, M.; Rudolfsen, G.; Munclinger, P.; Tucker, P.J.; Piálek, J. Sperm-related phenotypes implicated in both maintenance and breakdown of a natural species barrier in the house mouse. *Proc. Roy. Soc.* **2012,** *B 279*, 4803-4810. doi: 10.1098/rspb.2012.1802
2. Douglas-Hamilton, D.H.; Smith, N.G.; Kuster, C.E.; Vermeiden, J.P.W.; Althouse, G.C. Particle Distribution in Low-Volume Capillary-Loaded Chambers. *J Androl* **2005**, *26*, 107-114. doi: 10.1002/j.1939-4640.2005.tb02879.x

Kinetic Model of the Action of 17α-Ethynylestradiol on the Capacitation of Mouse Sperm, Monitored by HPLC-MS/MS

Tereza Bosakova [1], Antonin Tockstein [1], Natasa Sebkova [2], Radomir Cabala [1,3,*] and Katerina Komrskova [2,4,*]

[1] Department of Analytical Chemistry, Faculty of Science, Charles University, Albertov 2030, 128 43 Prague 2, Czech Republic; tereza.bosakova@natur.cuni.cz (T.B.); atockstein@seznam.cz (A.T.)
[2] Laboratory of Reproductive Biology, Institute of Biotechnology, Czech Academy of Sciences, BIOCEV, Prumyslova 595, 252 50 Vestec, Czech Republic; natasa.sebkova@ibt.cas.cz
[3] Toxicology Department, Institute of Forensic Medicine and Toxicology, General University Hospital in Prague, Ke Karlovu 2, 128 08 Prague 2, Czech Republic
[4] Department of Zoology, Faculty of Science, Charles University, Vinicna 7, 128 44 Prague 2, Czech Republic
* Correspondence: cabala@natur.cuni.cz (R.C.); katerina.komrskova@ibt.cas.cz (K.K.)

Abstract: 17α-Ethynylestradiol (EE2), a synthetic estrogen used in contraceptive pills, is resistant to hepatic degradation and is excreted in the urine. It is chemically stable and has a negative impact on the endocrine system. The aim of this work was to mathematically describe the possible interaction of EE2 (200, 20, and 2 μg/L) with sperm estrogen receptors during sperm maturation, which is called capacitation. The concentrations of the unbound EE2 remaining in capacitating medium during 180 min of sperm capacitation were determined at 30 min intervals by high performance liquid chromatography with tandem mass spectrometric detection (HPLC-MS/MS) and the data obtained (relative concentrations B_t) were subjected to kinetic analysis. The suggested kinetic schema was described by the system of differential equations with the optimization of rate constants used to calculate the theoretical B_t values. Optimal parameters (overall rate constants K_1–K_5 and molar ratio n) were determined by searching the minimum of absolute values of the difference between theoretical and experimental B_t values. These values were used for the design of the theoretical $B(t)$ curves which fit to experimental points. The proposed kinetic model assumes the formation of an unstable adduct between EE2 and the receptor in cytoplasm, which acts as an autocatalytic agent and gradually decomposes.

Keywords: 17α-ethynylestradiol; EE2; sperm capacitation; kinetics; autocatalysis; HPLC-MS/MS

1. Introduction

The estrogenic hormone 17α-ethynylestradiol (EE2) belongs to a group of pollutants termed estrogenic endocrine-disrupting chemicals (E-EDC), which are chemical substances in the environment that have a negative impact on the endocrine systems of animals and also humans [1]. E-EDCs enter the environment in the form of waste products as a result of elevated production and consumption of a number of drugs, e.g., hormonal contraceptives or supportive substances [2], and already constitute a toxicological reproductive risk at very low concentrations (ng/L). These substances can, in fact, simulate the behavior of endogenic estrogenic hormones, which control a number of physiological processes, including sperm maturation and preparation for fertilization, binding to their receptors [2–4] (estrogen receptors (ERs), nuclear receptors (nER), and membrane (mER) and cytoplasmic (cER) receptors) [5,6].

EE2 is a synthetic hormone used in hormonal contraception and is resistant to decomposition in the liver [7,8]. After ingestion, it is excreted in the urine, most often as a conjugate (glucuronate or sulphate), and thus enters waste waters, and, after deconjugation, can act as an E-EDC in the environment [9]. Its subsequent binding to an estrogen receptor can inhibit the secretion of the gonadotropin-releasing hormone and subsequently the secretion of the luteinizing hormone, leading to a reduction in the function or activity of the testes and directly affecting spermatogenesis, i.e., the process of formation and development of sperm, resulting in a male sex cell [10,11]. The sperm could then be morphologically mature, but not capable of fertilizing an egg [12].

Under normal circumstances, following ejaculation into the female reproductive system, sperm undergo complex biochemical and physiological changes, summarily termed capacitation [13]. Only capacitated sperm gain progressive motility (sperm hyperactivation) and are capable of penetrating through the egg envelope (in a process known as the acrosome reaction) and fertilizing the egg [14]. Capacitation in vivo, which includes membrane rearrangement, cholesterol efflux, activation of specific signal transduction pathways leading to protein tyrosine phosphorylation (TyrP) and cytoskeleton rearrangements [15–17], takes place in the uterus and fallopian tubes and is activated by substances excreted from the female genital tract. The capacitation process in vitro can take place under exactly delimited conditions employing incubation of sperm in a capacitation/fertilization medium containing albumin and calcium ions, at a temperature of 37 °C and in an atmosphere with 5% CO_2, which imitates the physiological environment in female genital tracts [15,18]. In order to study the effect of the presence of exogenous hormones on sperm capacitation in vitro, it is important to determine how capable the sperm is of binding these hormones during these processes and the dynamics of this process.

Methods of studying the effect of estrogenic hormones on sperm capacitation have been published only sporadically in the literature. Immunochemical methods have been used to study the effect of estrogens on the capacitation of mouse sperm in vivo [19] and boar sperm in vitro [20]. It has been found that sperm capacitation in vitro is substantially modulated by the presence of estrogens and that its speed can also be increased [21–23]. The effect of estriol on the capacitation of mouse sperm has been studied by HPLC with UV detection, but with low detection sensitivity [24]. The method was greatly improved by using sensitive HPLC-MS/MS methods for monitoring the action of 17β-estradiol (E2) on the capacitation of mouse sperm in vitro, enabling monitoring of changes in hormone concentration levels during sperm capacitation even at the level of units of μg/L [25,26], thus approaching real values of potential exposure. The obtained results were subjected to kinetic analysis, which has been used successfully to study the mechanism of the action of fluorides and aluminum fluoride complexes on the capacitation ability of mouse sperm [27]. The results of kinetic analysis of concentration changes on the receptors of unbound E2 during time-dependent sperm capacitation have demonstrated that E2 is first adsorbed on the surface of plasmatic membranes and subsequently passes into the cytoplasm, where it forms an unstable adduct with the receptors; the formation of this adduct has an autocatalytic effect [26]. It has thus been found that the application of kinetic analysis to the experimentally obtained data could be a useful instrument in monitoring sperm responses to the action of external factors and for prediction of kinetically specific mechanisms at a molecular level, including selected signal pathways.

This study focuses on the effect of synthetic EE2 on mouse sperm capacitation and comparison of the EE2 action with E2 [26]. An HPLC-MS/MS method capable of monitoring the concentration changes in unbound EE2 during time-dependent capacitation of mouse sperm in capacitating medium is developed, and the results obtained are subjected to kinetic analysis.

2. Results

2.1. HPLC-MS/MS Analysis

The ability of bovine serum albumin (BSA) to bind some estrogen substances, especially under in vitro conditions (tempering for 60 min in an incubator at 37 °C and 5% CO_2), has been described in

the literature [28–30]. Experiments were conducted to clarify whether EE2 is bound to BSA, and, if so, for how long. Consequently, samples were taken at times of 0, 30, 60, and 90 min during tempering of EE2 in the capacitating medium (200, 20, and 2 µg/L) under in vitro conditions and were subsequently analyzed by the developed HPLC-MS/MS method. It was found that the EE2 concentration decreases during tempering. If the values of the relevant concentrations are compared at the start (200, 20, and 2 µg/L) and after 60 min (~180, 18, and 1.8 µg/L) of tempering, it can be seen that their differences (~20, 2, and 0.2 µg/L) decrease with decrease in the initial EE2 concentration following the concept of simple equilibrium. The EE2 concentration decreases especially in the first 30 min and then remains practically constant up to 90 min, which means that after 30 min no EE2 binds to BSA. This is very important because at 60 min, when tempering of the prepared biological samples is terminated, the sperm are immediately added to the sample and their capacitation begins.

The process of capacitation was monitored for the time range 0 to 180 min with a 30 min interval between sample collections. The biological sample (EE2 in capacitating medium with the addition of sperm) was measured in three parallel sets ($n' = 3$) where each set represented sperm collected from one individual. Blanks (no sperm) were also prepared for each tested concentration. The course of the entire measurement for the tested EE2 concentrations is depicted in Figure 1A–C. It can be seen in Figure 1A–C that there is a gradual decrease in the concentration of EE2 in the time interval 0 to 60 min, with a minimum value on the curve at around 60 min of capacitation for all the measured concentrations (200, 20, and 2 µg/L). This means that the greatest binding of the hormone by sperm occurred around 60 min of capacitation. Subsequently, after the first decrease, the hormone concentration increased until the end of capacitation, i.e., to 180 min, when the concentration of the overall unbound EE2 approached the original concentration value at time 0 min. This gradual increase in concentration was caused by the slow release of EE2 bound in the sperm. On the other hand, analysis of the blank samples demonstrated that the EE2 concentration was practically constant for the whole measured time. For comparison of the results obtained for various dilutions of EE2 (concentrations 200, 20, and 2 µg/L) it is useful to introduce relative values of B_t, calculated as $C_{(t)}/C_{(t=0)}$ (for the individual capacitation times), which are listed in Table 1.

Table 1. Relative concentration B_t calculated from the means of measured EE2 time-dependent concentrations C ($n' = 3$) obtained during capacitation for three tested EE2 concentrations (see Figure 1).

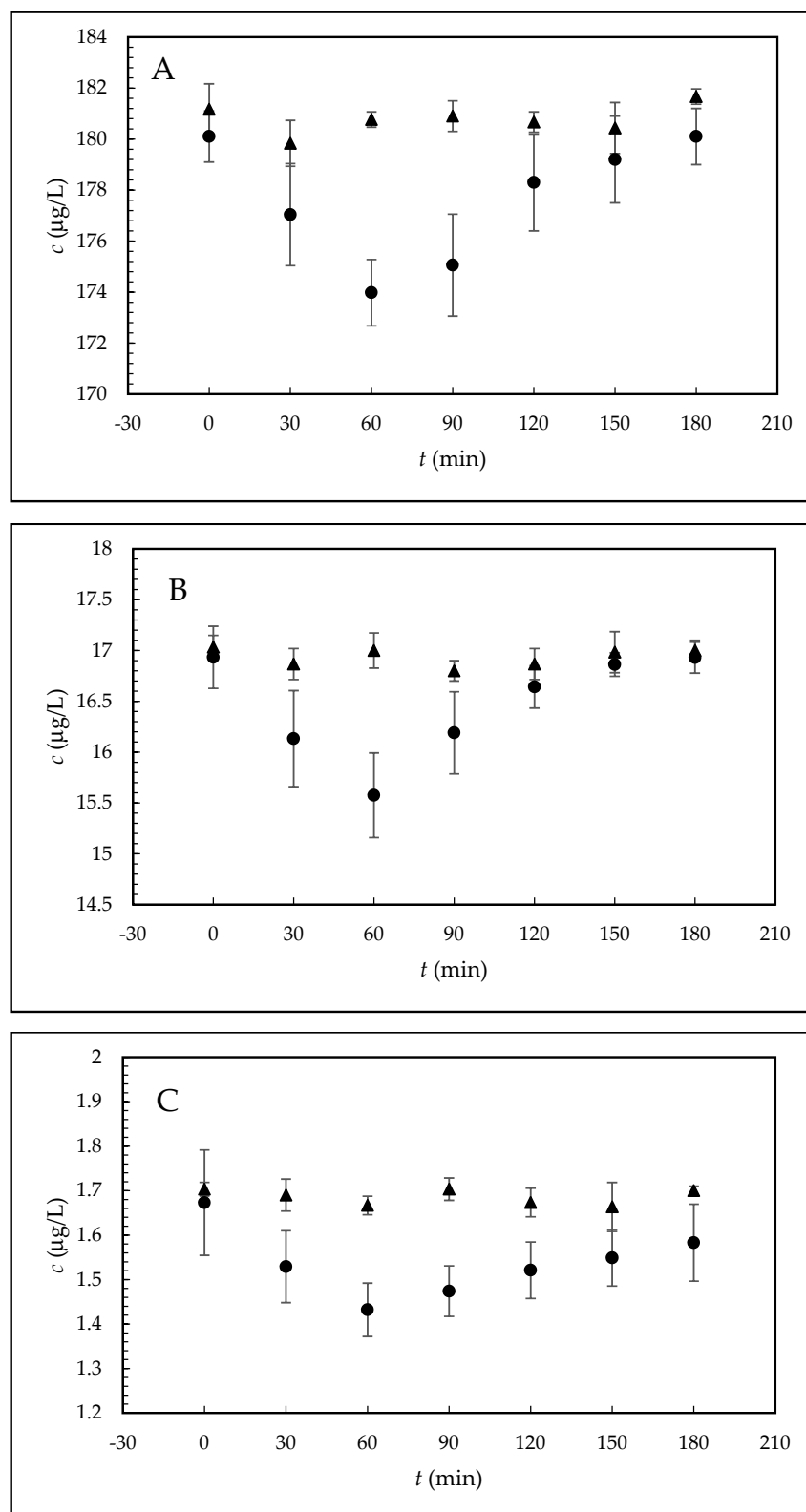| Capacitation Time (min)	B_t		
	200 µg/L	20 µg/L	2 µg/L
0	1.000	1.000	1.000
30	0.983	0.953	0.914
60	0.966	0.920	0.856
90	0.972	0.956	0.881
120	0.990	0.983	0.909
150	0.994	0.996	0.926
180	1.000	1.000	0.946

Figure 1. Dependencies of the concentration of the overall unbound 17α-ethynylestradiol (EE2) on the time of mouse sperm capacitation in vitro. The tested concentrations of EE2 in the capacitating medium were (**A**) 200 μg/L, (**B**) 20 μg/L, and (**C**) 2 μg/L. The samples were prepared in three parallel sets, where each set represented sperm collected from one individual (dots). The blanks were prepared and measured in parallel (triangles). Experimental conditions: 50/50 (*v/v*) acetronitrile (ACN)/H_2O, both containing 0.1% formic acid (HCOOH), measured in the multiple reaction monitoring (MRM) mode for transition 279.1 → 133.0; the error bars were calculated using the standard deviations ($n' = 3$).

2.2. Kinetic Analysis of the HPLC-MS/MS Data

The obtained HPLC-MS/MS data was subjected to kinetic analysis to determine the mechanism of EE2 action on sperm during their capacitation. The curve interposed by the experimentally measured points (concentration of unbound EE2 in dependence on the time of sperm capacitation (Figure 1)), exhibited an autocatalytic character. This followed from two parameters: the slope (tangent) of the dependence of the measured quantity on time became steeper during the interaction, i.e., the interaction rate increased, and the hormone (EE2) formed an adduct (EE2-R) with the receptor (R). However, the adduct was unstable and subsequently decomposed, increasing the concentration of unbound EE2. The concept of the autocatalytic course is based on the fact that similar behavior has already been described for E2 [26]. This means that the initial formation of the adduct (non-catalytic step) leads to increased accessibility of the cytoplasmic membrane (termed signaling). The energy released in the formation of bonds between the receptor and the hormone is transferred by the bond system of the macromolecular receptors to the surface of the membrane, where it causes relaxation of this membrane and becomes more permeable for the passage of a higher amount of extracellular EE2 (autocatalytic step).

Four hypothetical possibilities can be considered to describe the decomposition of the adduct located inside the cytoplasmic membrane of sperm: (i) the decomposition produces active EE2$_i$ and active R, both capable of further interactions; (ii) the decomposition produces active EE2$_i$ and inactive receptor R′; (iii) the decomposition produces active receptor R and inactive hormone EE2$_i$′; and (iv) the decomposition yields both inactive products, i.e., R′ and EE2$_i$′. The last two reactions (iii) and (iv) can be rejected because it follows from the experimental data that at the end of the interaction between the hormone and sperm, the hormone returns to its starting concentration. Thus, we can consider reactions (i) and (ii) only. Because both of the components formed in the first reaction (i) are active, it is easy to imagine a reverse back (equilibrium) reaction between the hormone and the receptor in the cytoplasm. On the other hand, the second reaction (ii) is unidirectional and leads to deactivation of the receptor. The two reactions, (i) and (ii), can take place simultaneously and this phenomenon can be considered as a disturbance of the equilibrium (i.e., a pseudo-equilibrium reaction). The whole process can be described by the simple scheme shown in Figure 2. It follows from the scheme that monitoring of the EE2 concentration by HPLC/MS-MS (described in Section 2.1) is related to the overall concentration of free, unbound hormone, i.e., the original EE2 and the internal EE2$_i$. After centrifugation, both components of the hormone are present in the supernatant; on the other hand, the hormone bound in the complex with the receptor (adduct: EE2-R) remains in the sediment and its concentration is not measured.
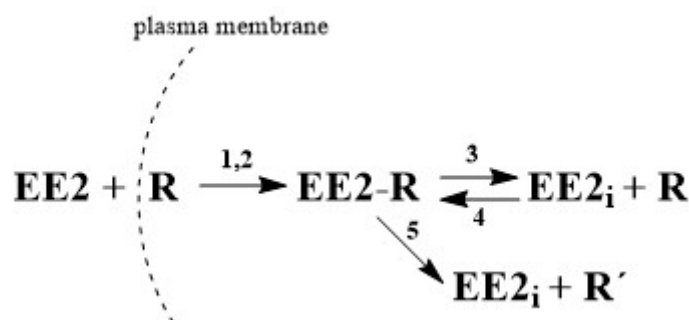

Figure 2. Simplified process of the interaction between hormone and sperm receptor, where EE2 is the extracellular hormone, R is the active sperm receptor, EE2-R is the adduct, EE2$_i$ is the internal unbound hormone and R′ is the inactive sperm receptor; 1 and 2 represent rate constants of the non-autocatalytic (1) and autocatalytic (2) formation of EE2-R which are ongoing simultaneously, 3 and 5 represent rate constants of adduct decomposition, and 4 represents the rate constant of the back reaction.

Furthermore, the kinetic scheme describes kinetic products and rate constants (K_1–K_5) in the form of the following rate equations. For brevity, the term EE2 is replaced in the equations by the symbol

E, also designating its molar concentration under various experimental conditions. *R* designates the receptor and its concentration, the symbol *ER* stands for the adduct, E_i is the internal free hormone in the cytoplasm, and ε is the relative concentration of unbound hormone outside the membrane.

$$\frac{-dE}{dt} = E \times R(K_1 + K_2 \times (1 - \varepsilon)) \tag{1}$$

$$\frac{-dR}{dt} = E \times R(K_1 + K_2 \times (1 - \varepsilon)) + K_4 \times E_i \times R - K_3 \times (ER) \tag{2}$$

$$\frac{d(ER)}{dt} = E \times R(K_1 + K_2 \times (1 - \varepsilon)) + K_4 \times E_i \times R - (K_3 + K_5) \times (ER) \tag{3}$$

Equation (1) describes the decrease in hormone *E* on reaction with receptor *R* by non-autocatalytic (K_1) and autocatalytic (K_2) reactions, Equation (2) describes the decrease in the receptor through its reaction with the external (K_1, K_2) and internal hormone (K_4) and increase by the adduct decomposition (K_3), and Equation (3) describes the increase in the adduct through the non-autocatalytic (K_1), autocatalytic (K_2), and back (K_4) reactions and decrease through the equilibrium (K_3) and pseudo-equilibrium (K_5) reactions. The derivation of the individual differential equations and reasons for their specific position are described in detail in Section 4.4.

The parameters of the theoretical $B(t)$ curves, i.e., the rate constants K_0–K_5 and the molar ratio *n*, were optimized by looking for the minima in the absolute values of the difference between the theoretical and experimental B_t values using the Matlab program. The results of optimization of the rate constants and parameter *n* are listed in Table 2, and Figure 3 shows very good agreement between the theoretical curves and the experimental points.

Table 2. Calculated constants for three tested EE2 concentrations, where *C* is the tested concentration, *n* is the molar ratio, K_1–K_5 are the overall rate constants, K_0 is the basic rate constant of the first step in the formation of the adduct, and R_0 is the number of total receptors.

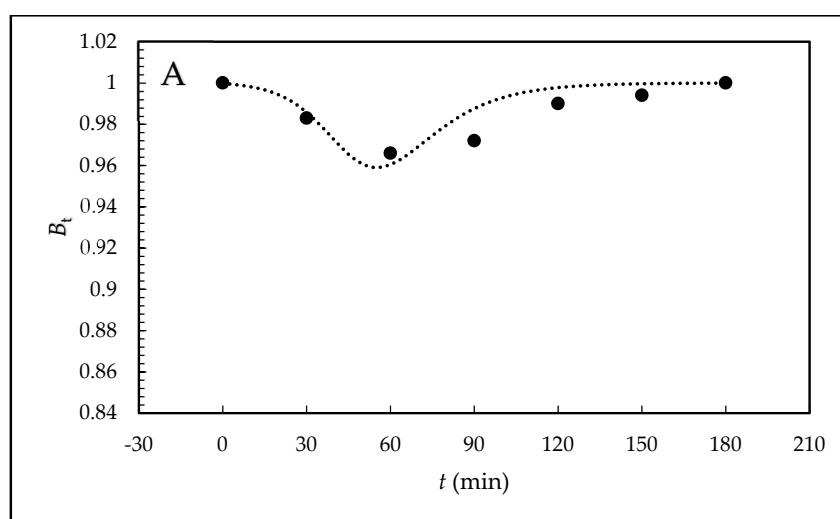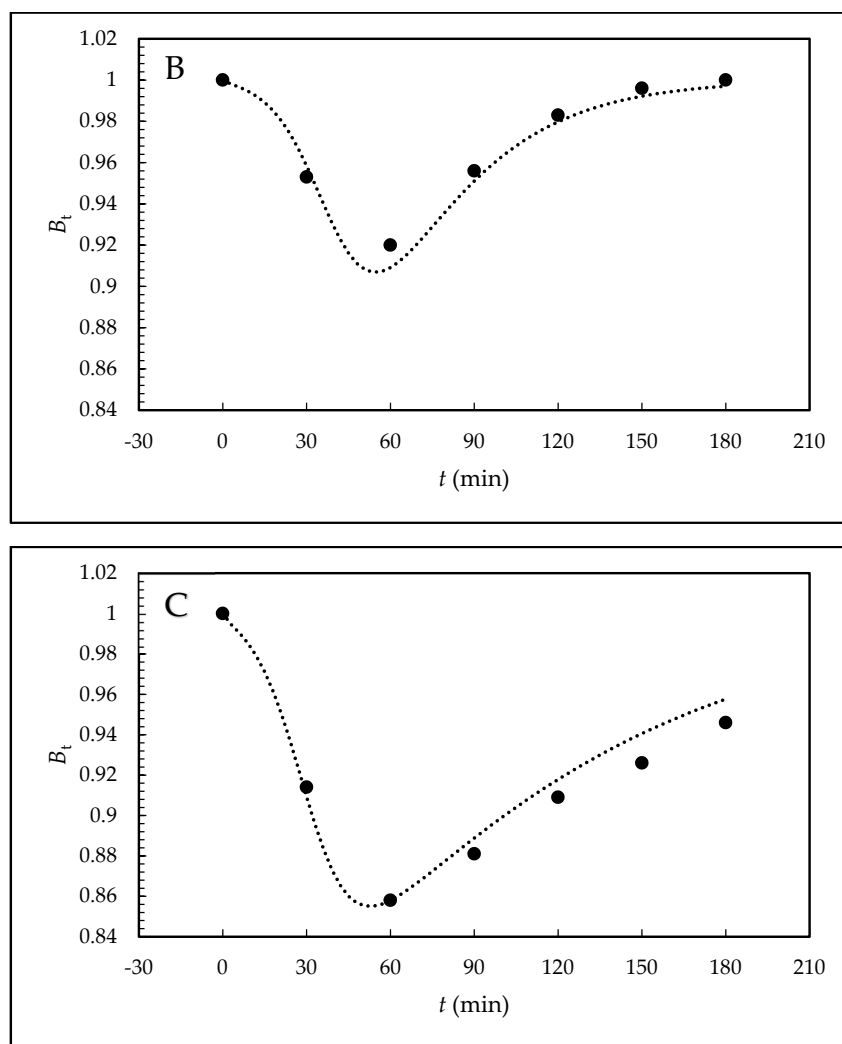| *C* (µg/L)	$K_1 = K_0/n$	K_2	$K_3' = (K_3 + K_5)/R_0$	K_4	$K_5' = K_5/R_0$	*n*	$K_0 = K_1 \cdot n$
200	0.029	10	49	12	20	2.44	0.0725
20	0.098	10	49	12	20	0.770	0.0734
2	0.270	10	49	12	20	0.265	0.0715

Figure 3. *Cont.*

Figure 3. Theoretical shape of the $B(t)$ curves obtained by integration of the kinetic equations for the selected concentrations (**A**) 200 µg/L, (**B**) 20 µg/L, and (**C**) 2 µg/L, molar ratios n, and optimized values of K_1–K_5 (see Table 3) with designation of the B_t points obtained in the experiment (see Table 2).

3. Discussion

The results show that with the simultaneous progress of the equilibrium and pseudo-equilibrium reactions, the course of the $B(t)$ curves can be described over almost two concentration orders simply by a change in parameter n with unvarying rate constants. This is perfect behavior in which the description of the kinetic scheme reflects its suitability. The correctness of the proposed model is further confirmed by the positions of the minima on the $B(t)$ curves, which are in agreement with the experimental values. The kinetic model and positions of the individual kinetic equations demonstrate that EE2 binds rapidly to the receptors but that this is a very weak bond. This also corresponds to the character of the values of the decomposition rate constants, which are larger than the rate constants of adduct formation. The adduct is unstable and is connected with inactivation of the binding receptor. The back reaction progresses relatively easily.

The theoretical shape of the $B(t)$ curves obtained for synthetic EE2 mimics behavior of endogenic E2 [26]; this means that the course has similar autocatalytic character. The differences between these two hormones are in the position of the minimum of curves. In the case of EE2 the minimum remains at the constant position of capacitation time (60 min) and does not depend on the tested concentration. On the other hand, with increasing E2 concentration, the position of the minimum value shifts to

longer times (from 30 min for 200 µg/L to 90 min for 2 µg/L) as a result of initial adsorption of E2 on the plasma membrane surface controlled by the Langmuir isotherm.

4. Materials and Methods

4.1. Chemicals, Reagents, and Animals

Acetonitrile (ACN) for LC-MS, Chromasolv (purity ≥ 99.9%), deuterated β-estradiol-16,16,17-d3 (estradiol-d3) (purity 98%), and commercial capacitating M2 culture media for in vitro sperm capacitation and fertilization (M7167) were purchased from Sigma-Aldrich (Steinheim, Germany). Ethanol (purity ≥ 96% p.a.) was obtained from Lachner (Neratovice, Czech Republic). Paraffin oil was provided by Carl Roth (Karlsruhe, Germany). Formic acid (HCOOH) (purity 98% p.a.) and 17α-ethynylestradiol (purity 98%) were obtained from Merck (Darmstadt, Germany). Deionized water (1.85 µS, Milli-Q water purification system Millipore, Burlington, MA, USA) was used in all the experiments.

Laboratory inbred strain of house mouse BALB/c was used for the experiments. The mice were housed in animal facilities of the Institute of Molecular Genetics of Czech Academy of Science, Prague, and food and water were supplied ad libitum. All the animal procedures and all the experimental protocols were approved by the Animal Welfare Committee of the Czech Academy of Sciences (Animal Ethics Number 66866/2015-MZE-17214, 18 December 2015).

4.2. Instrumentation and Chromatographic Conditions

The HPLC equipment (Agilent Technologies, Waldbronn, Germany) consisted of a 1290 Infinity Series LC (a quaternary pump, degasser, thermostatic auto sampler, and column oven). A Triple Quad LC/MS 6460 tandem mass spectrometer (Agilent Technologies, Waldbronn, Germany) with an electrospray ionization interface was used for the detection. The signal was processed and data were handled using MassHunter Workstation Acquisition and MassHunter Qualitative Analysis Software (Agilent Technologies, Waldbronn, Germany).

All the instrumental MS-MS parameters were optimized. ESI (+) conditions in the MRM mode for EE2 were capillary voltage 4000 V, nebulizer pressure 55 psi, gas temperature 350 °C, and nitrogen flow rate 10 L/min. For EE2 the m/z 279.1 → 133.0 transition (fragmentor voltage 100 V, collision energy 15 V, and parameter dwell 400 ms) and for estradiol-d3 the m/z 258.5 → 158.9 transition (fragmentor voltage 100 V, collision energy 15 V, and parameter dwell 400 ms) were monitored, respectively.

The separation system was based on the publication of Bosakova et al. [26] with a Kinetex EVO column C18 (100 × 3.0 mm, 2.6 µm, Phenomenex, Torrance, CA, USA) and a mobile phase containing a binary mixture of ACN/water with addition of 0.1% HCOOH in both parts at a volume ratio of 50/50 (*v/v*); the flow rate was 0.3 mL/min. The column temperature was held at 21 ± 0.5 °C. The amount of sample injected equaled 7.5 µL. Estradiol-d3, which was used as an internal standard (IS) at a final concentration of 25 µg/L (diluted in capacitating medium) was added to each sample. The retention times of IS and EE2 were 3.1 and 3.7 min, respectively. Because of the complex capacitating medium containing inorganic and organic components, of which especially bovine serum albumin (4.0 g/L) can cause difficulties during the separation and detection processes, the eluate was fed to waste from 0 to 2.5 min and to the MS detector only from 2.5 to 5.0 min.

The linearity of the method was determined from the calibration curve constructed by plotting the ratio of the peak areas of EE2 to that of IS against the analyte concentration. It was statistically analyzed by 1/x weighted linear regression analysis using the least-squares regression method. The obtained data was linear (y = 0.0252x − 0.0298, R^2 = 0.9989) in the whole measured calibration range 1–225 µg/L. Relative standard deviations (*n'* = 5) varied from 1.8–3.3%. The limit of detection (0.88 µg/L) and limit of quantitation (1.21 µg/L) were calculated as the 3.3 × σ/S and 10 × σ/S ratios, respectively, where σ was the baseline noise of the sample and *S* was the slope of the regression curve (based on peak heights) constructed from the calibration curve. The accuracy, precision, and repeatability were

measured at three EE2 concentration levels (200, 20, and 2 µg/L). Intra-day and inter-day accuracy and precision (each $n' = 5$) were determined by repeatedly assaying samples on the same day and on two consecutive days, respectively. The results are summarized in Table 3.

Table 3. Validation parameters for intra-day and inter-day accuracy and precision ($n' = 5$).

C (Theoretical) (µg/L)	Intra-Day (µg/L)	Accuracy (%)	Precision (%)	Inter-Day (µg/L)	Accuracy (%)	Precision (%)
200	202.1 ± 0.2	101.1	1.07	203.3 ± 0.4	101.6	1.63
20	19.9 ± 0.01	99.5	0.55	19.8 ± 0.1	99.1	0.90
2	1.9 ± 0.01	97.0	3.00	1.91 ± 0.04	95.5	4.50

4.3. Capacitation of Mouse Sperm In Vitro

Thirty-five millimeter Petri dishes obtained from Thermo Fisher Scientific (Rochester, NY, USA) were used for the capacitation in vitro. An Olympus CX 21 inverted-light microscope and Olympus epifluorescent microscope were supplied by Olympus (Prague, Czech Republic). An NB-203 incubator was purchased from N-BIOTEK (Gyeonggi-do, Korea). A Telstar Bio-IIA incubator and BioTek laminar box from N-BIOTEK (Gyeonggi-do, Korea) were used for the in vitro sperm cultivation.

Firstly, a stock solution of the EE2 standard with a concentration of 200 mg/L was prepared in ethanol, from which working ethanol solutions of EE2 with concentrations of 20 and 2 mg/L were diluted. In the laminar box, 1 µL of the working ethanol solution of EE2 with the appropriate concentration (200, 20, or 2 mg/L) was pipetted, diluted by capacitating medium to a volume of 1 mL in the test tube so that the final test concentration of EE2 in the capacitating medium was obtained (200, 20, or 2 µg/L), and the ethanol content was minimized and remained constant. Subsequently, 100 µL of solution with the appropriate concentration was pipetted into the fertilization Petri dish. The pipetted mixture in the Petri dish was covered with 1 mL of paraffin oil. The prepared Petri dishes were placed in the incubator and tempered for 60 min at a temperature of 37 °C and with 5% CO_2 in the air.

The spermatozoa which were recovered from the distal region of the *cauda epididymidis* were placed in the fertilization Petri dishes with capacitating medium and paraffin oil and then placed for 10 min in the incubator for sperm release. Then, the stock concentration of mouse sperm was adjusted to 5×10^6 sperm/mL. During preparation, the motility of the sperm was controlled under a microscope.

The biological sample was prepared as follows. Following 60 min of tempering, 5 µL of the stock sperm were added to 100 µL of the EE2 sample in capacitating medium (200, 20, or 2 µg/L). For each capacitation time (0–180 min) eight Petri dishes containing 105 µL of sample covered with 1 mL of paraffin oil were prepared. The dishes prepared in this way were incubated again under the same conditions for various time periods (0, 30, 60, 90, 120, 150, and 180 min after adding the sperm), during which sperm capacitation took place. After the individual times, samples (only the solutions with the capacitating medium and without the paraffin oil), were pipetted from all eight Petri dishes into a single micro-test tube, which was centrifuged for 10 min at 12,000 rpm. In this way the sperm were separated from the solution and approximately 600 µL of supernatant was obtained for HPLC-MS/MS analysis of free, sperm-unbound EE2. This sample represented one sampling time during capacitation.

In order to eliminate any systematic errors during sample preparation (e.g., partial evaporation of samples during incubation or differences in collection of the supernatant after centrifugation, etc.), reference samples (blanks) without addition of mouse sperm were prepared simultaneously under the same experimental conditions.

Prior to the actual HPLC-MS/MS analysis, 20 µL of estradiol-d3 (IS) with a concentration of 250 µg/L was added to each biological sample as well as to each blank (180 µL).

The matrix effect was investigated by comparison of the results (EE2/IS peak area ratios) obtained for samples prepared by two different procedures: (i) the sample was prepared by addition of EE2 and IS to the supernatant, which was obtained after the capacitating medium with sperm covered with paraffin oil was tempered, the paraffin oil removed, and the capacitating medium centrifuged; (ii) the

sample was prepared by addition of EE2 and IS to the capacitating medium. Each experiment was performed in triplicate for all EE2 concentrations (200, 20, and 2 µg/L). The recovery percentages of the samples with EE2 concentrations of 200, 20, and 2 µg/L were 94.3, 97.1, and 95.8%, respectively.

4.4. Mathematical Model

As was described in Section 2.2, the term EE2 has been replaced in equations with the symbol E, which also designates its molar concentration under various experimental conditions. R designates the receptor and its concentration, symbol ER stands for the adduct, E_i is the internal free hormone in the cytoplasmic membrane, and R' is the inactive receptor. The formation of the ER adduct following the interaction of hormone E with receptor R on the sperm leads to relaxation of the cytoplasmic membrane.

Because the amount of adduct formed is proportional to the difference $E_{(t=0)} - E_{(t)}$ and because the amount of hormone at the end of the reaction equals 0, the degree of relaxation of membrane S can be defined as $\frac{E_{(t=0)} - E_{(t)}}{E_{(t=0)}}$, meaning $S = 1 - \varepsilon$, where ε is the relative concentration of unbound hormone outside the membrane. Autocatalytic formation of the adduct thus progresses with rate "constant" $k_1 + S \times k_2 = k_1 + k_2 \times (1 - \varepsilon)$.

Taking into consideration all the possibilities, this can be described by the following system of kinetic equations, i.e., Equations (1)–(7).

$$\frac{dE_i}{dt} = (K_3 + K_5) \times (ER) - (K_4 \times E_i \times R) \tag{4}$$

$$\frac{dR'}{dt} = K_5 \times (ER) \tag{5}$$

Equation (1) describes the decrease in hormone E by reaction with receptor R by non-autocatalytic (K_1) and autocatalytic (K_2) reactions, Equation (2) describes the decrease in the receptor through its reaction with the external (K_1, K_2) and internal hormone (K_4) and increase by the adduct decomposition (K_3), and Equation (3) describes the increase in the adduct through the non-autocatalytic (K_1), autocatalytic (K_2), and back (K_4) reactions and decrease through the equilibrium (K_3) and pseudo-equilibrium (K_5) reactions. Equation (4) describes the increase of the internal hormone E_i by the adduct decomposition (K_3 and K_5) and its decrease by back K_4 reaction. Equation (5) describes the formation (K_5) of inactive receptor R'.

The balance equation for the hormone (Equation (6)) and the balance equation for the receptor (Equation (7)) are valid, i.e.,

$$E_o = E + (ER) + E_i \text{ so that } E_i = E_o - E - (ER) \tag{6}$$

$$R_o = R + (ER) + R' \text{ so that } R = R_o - (ER) - R' \tag{7}$$

In the kinetic equations, E_i and R can be expressed according to Equations (6) and (7), meaning the set of kinetic equations is reduced to three for variables E, (ER), and R'.

Further, the relative variables are introduced, i.e.,

$$\frac{E}{E_o} = \varepsilon \quad \frac{(ER)}{E_o} = \alpha \quad \frac{E_o}{R_o} = n \quad \frac{R'}{R_o} = \beta \tag{8}$$

Equation (8) can also be used to describe the relative concentration of the internal hormone $\frac{E_i}{E_0}$ and the relative concentration of the receptor $\frac{R}{R_0}$ in Equations (6) and (7).

$$\frac{E_i}{E_o} = 1 - \varepsilon - \alpha \quad \frac{R}{R_o} = 1 - \frac{(ER)}{R_o} - \frac{R'}{R_o} \text{ so that } \frac{R}{R_o} = 1 - \alpha \times n - \beta \tag{9}$$

Introduction of the relative concentrations and generalized time $\tau = R_0 \times t$ yields a set of three differential equations, Equations (10)–(12), i.e.,

$$\frac{-d\varepsilon}{dT} = (K_1 + K_2 \times (1 - \varepsilon)) \times (1 - n \times \alpha - \beta) \times \varepsilon \tag{10}$$

$$\begin{aligned}\frac{d\alpha}{dT} = {}&(K_1 + K_2 \times (1 - \varepsilon)) \times (1 - n \times \alpha - \beta) \times \varepsilon - \left(\frac{K_3}{R_o} + \frac{K_5}{R_o}\right) \times \alpha \\ &+ K_4(1 - \varepsilon - \alpha) \times (1 - n \times \alpha - \beta)\end{aligned} \tag{11}$$

$$\frac{d\beta}{dT} = n \times \alpha \times \frac{K_5}{R_o} \tag{12}$$

where the definitions of $K_3{}'$ and $K_5{}'$ are

$$\frac{K_3}{R_0} = K_3{}'; \quad \frac{K_5}{R_0} = K_5{}' \tag{13}$$

Furthermore, the kinetic scheme employs kinetic products and rate constants in the form of rate equations. The relative values are introduced for the individual variables and the system is solved by numerical integration with simultaneous optimization of the rate constants, including parameter n. Because the sum of the relative concentrations of free hormone B and sperm-bonded hormone α must equal 1, B equals 1–α. Quantity B can be measured and also theoretically calculated from α. For the given kinetic scheme, comparison of the theoretical values with the experimental values makes it possible to decide whether the proposed kinetic scheme is credible.

The equations are solved by the fourth-order Runge-Kutta method with step of $h = 10^{-4}$. The parameters of the theoretical $B(t)$ curves, i.e., the rate constants and the molar ratio n, were optimized by looking for the minima of the absolute values of the difference between the theoretical and experimental B_t values. The obtained constant values are given in Table 2 and the shapes of the theoretical curves are depicted in Figure 3.

5. Conclusions

In this work, an HPLC-MS/MS method was developed and validated for analysis of EE2 concentration in capacitating medium. This method was subsequently used to monitor the concentration changes of the free hormone not bound by mouse sperm during time-dependent capacitation. The experimentally (HPLC-MS/MS) obtained B_t data were subjected to kinetic analysis and the kinetic model, described by three principal kinetic equations, was designed as follows. Extracellular EE2 can bind to the plasma membrane receptors, forming the adduct in cytoplasm. Once formed, the adduct serves as an autocatalytic agent, acting on the plasma membrane to increase its fluidity. This leads to an increase in the interaction rate between the hormone and the receptor in the cytoplasm. However, the formed adduct is unstable and gradually decomposes. The decomposition can produce the active form of the internal hormone (EE2$_i$) and active receptor (R) in the cytoplasm, which are both capable of further interactions, enabling a reverse back (equilibrium) reaction. The decomposition can also lead to the deactivation of the receptor (R′) during a unidirectional reaction. Both reactions can take place simultaneously and can be considered to be a pseudo-equilibrium reaction (Figure 2). The monitoring of EE2 concentration by HPLC/MS-MS in capacitating medium is related to the overall concentration of free unbound hormone, i.e., the original extracellular EE2 together with the internal EE2$_i$. After centrifugation, both components of the hormone are present in the supernatant, but on the other hand, the hormone bound in the complex with the receptor (adduct: EE2-R) remains in the sediment and its concentration is not measured. Very good agreement of the experimental B_t values with the theoretically calculated values confirms that the proposed kinetic scheme is credible.

The theoretical shape of the $B(t)$ curves obtained for synthetic EE2 mimics behavior of endogenic E2 [26]; this means that the course has similar autocatalytic character. The differences between EE2 and E2 are in the position of the minimum of $B(t)$ curves for the increased initial tested concentration

of these two hormones. For EE2, it remains at a constant position of capacitation time and does not depend on the tested concentration. On the other hand, with the increasing E2 concentration, the position of the minimum value shifts to longer times as a result of initial adsorption of E2 on the plasma membrane surface controlled by the Langmuir isotherm. The results suggest that this new analytical–mathematical approach to reproductive biology, such as the study of the mechanism of action of steroid hormones on sperm capacitation, is of a more general nature and can be used in a broader context of endocrine signaling.

Author Contributions: T.B. performed the HPLC-MS/MS experiments and the relevant statistics; T.B., A.T., and R.C. designed and performed the kinetic analysis and wrote the relevant part of the manuscript; N.S. performed sperm capacitation; and K.K. designed and supervised the biological part of the project, including sperm capacitation, analyzed the data, and wrote the relevant parts of the manuscript. All authors have read and agreed to the published version of the manuscript.

Conflicts of Interest: The authors declare no conflict of interest.

References

1. Campbell, C.G.; Borglin, S.E.; Green, F.B.; Grayson, A.; Wozei, E.; Stringfellow, W.T. Biologically directed environmental monitoring, fate, and transport of estrogenic endocrine disrupting compounds in water: A review. *Chemosphere* **2006**, *65*, 1265–1280. [CrossRef] [PubMed]

2. López de Alda, M.J.; Barceló, D. Determination of steroid sex hormones and related synthetic compounds considered as endocrine disruptors in water by liquid chromatography-diode array detection-mass spectrometry. *J. Chromatogr. A* **2000**, *892*, 391–406. [CrossRef]

3. Colborn, T.; vom Saal, F.S.; Soto, A.M. Developmental effects of endocrine-disrupting chemicals in wildlife and humans. *Environ. Health Perspect.* **1993**, *101*, 378–384. [CrossRef] [PubMed]

4. Della Seta, D.; Farabollini, F.; Dessí-Fulgheri, F.; Fusani, L. Environmental-like exposure to low levels of estrogen affects sexual behavior and physiology of female rats. *Endocrinology* **2008**, *149*, 5592–5598. [CrossRef] [PubMed]

5. Aquila, S.; De Amicis, F. Steroid receptors and their ligands: Effects on male gamete functions. *Exp. Cell Res.* **2014**, *328*, 303–313. [CrossRef] [PubMed]

6. Dostalova, P.; Zatecka, E.; Dvorakova-Hortova, K. Of Oestrogens and perm: A Review of the roles of oestrogens and oestrogen receptors in male reproduction. *Int. J. Mol. Sci.* **2017**, *18*, 904. [CrossRef]

7. Matějíček, D.; Kubáň, V. High performance liquid chromatography/ion-trap mass spectrometry for separation and simultaneous determination of ethynylestradiol, gestodene, levonorgestrel, cyproterone acetate and desogestrel. *Anal. Chim. Acta* **2007**, *588*, 304–315. [CrossRef]

8. Ingrand, V.; Herry, G.; Beausse, J.; de Roubin, M.R. Analysis of steroid hormones in effluents of wastewater treatment plants by liquid chromatoraphy–tandem mass spectrometry. *J. Chromatogr. A* **2003**, *1020*, 99–104. [CrossRef]

9. Čelić, M.; Biljana, S.I.; Petrović, M. Development of a sensitive and robust online dual column liquid chromatography-tandem mass spectrometry method for the analysis of natural and synthetic estrogens and their conjugates in river water and wastewater. *Anal. Bioanal. Chem.* **2017**, *409*, 5427–5440. [CrossRef]

10. Safe, S.H.; Pallaroni, L.; Yoon, K.; Gaido, K.; Ross, S.; Saville, B.; McDonnellc, D. Toxicology of environmental estrogens. *Reprod. Fertil. Dev.* **2001**, *13*, 307–315. [CrossRef] [PubMed]

11. Kumar, V.; Majumdar, C.; Roy, P. Effects of endocrine disrupting chemicals from leather industry effluents on male reproductive system. *J. Steroid Biochem. Mol. Biol.* **2008**, *111*, 208–216. [CrossRef] [PubMed]

12. Yoshida, M.; Kawano, N.; Yoshida, K. Control of sperm motility and fertility: Diverse factors and common mechanisms. *Cell. Mol. Life Sci.* **2008**, *65*, 3446–3457. [CrossRef] [PubMed]

13. Yanagimachi, R. Mammalian fertilization. In *The Physiology of Reproduction*; Knobil, E., Neill, J.D., Eds.; Raven Press: New York, NY, USA, 1994; pp. 189–317.

14. Suarez, S.S.; Pacey, A.A. Sperm transport in the female reproductive tract. *Hum. Reprod. Update* **2006**, *12*, 23–37. [CrossRef]

15. Naz, R.K.; Rajesh, P.B. Role of tyrosine phosphorylation in sperm capacitation/acrosome reaction. *Reprod. Biol. Endocrin.* **2004**, *2*, 75–87. [CrossRef] [PubMed]

16. Visconti, P.E.; Bailey, J.L.; Moore, G.D.; Pan, D.; Olds-Clarke, P.; Kopf, G.S. Capacitation of mouse spermatozoa. I. Correlation between the capacitation state and protein tyrosine phosphorylation. *Development* **1995**, *121*, 1129–1137. [PubMed]

17. Wang, J.; Qi, L.; Huang, S.; Zhou, T.; Guo, Y.; Wang, G.; Guo, X.; Zhou, Z.; Sha, J. Quantitative phosphoproteomics analysis reveals a key role of insulin growth factor 1 receptor (IGF1R) tyrosine kinase in human sperm capacitation. *Mol. Cell. Proteom.* **2015**, *14*, 1104–1112. [CrossRef]

18. Huang, T.T.; Fleming, A.D.; Yanagimachi, R. Only acrosome-reacted spermatozoa can bind to and penetrate zona pellucida: A study using the guinea pig. *J. Exp. Zool.* **1981**, *217*, 287–290. [CrossRef]

19. Ded, L.; Sebková, N.; Cerna, M.; Elzeinova, F.; Dostalova, P.; Peknicova, J.; Dvorakova-Hortova, K. In vivo exposure to 17β-estradiol triggers premature sperm capacitation in cauda epididymis. *Reproduction* **2013**, *145*, 255–263. [CrossRef]

20. Děd, L.; Dostálová, P.; Dorosh, A.; Dvořáková-Hortová, K.; Pěknicová, J. Effect of estrogens on boar sperm capacitation in vitro. *Reprod. Biol. Endocrinol.* **2010**, *8*. [CrossRef]

21. Peknicová, J.; Kyselová, V.; Boubelík, M.; Buckiová, D. Effect of an endocrine disruptor on mammalian fertility. Application of monoclonal antibodies against sperm proteins as markers for testing sperm damage. *Am. J. Reprod. Immunol.* **2002**, *47*, 311–318. [CrossRef]

22. Baldi, E.; Luconi, M.; Muratori, M.; Marchiani, S.; Tamburrino, L.; Forti, G. Nongenomic activation of spermatozoa by steroid hormones: Facts and fictions. *Mol. Cell. Endocrinol.* **2009**, *308*, 39–46. [CrossRef] [PubMed]

23. Sebkova, N.; Cerna, M.; Ded, L.; Peknicova, J.; Dvorakova-Hortova, K. The slower the better: How sperm capacitation and acrosome reaction is modified in the presence of estrogens. *Reproduction* **2012**, *143*, 297–307. [CrossRef] [PubMed]

24. Dvořáková-Hortová, K.; Honetschlägerová, M.; Tesařová, E.; Vašinová, J.; Frolíková, M.; Bosáková, Z. Residual concentration of estriol during mouse sperm capacitation in vitro determined by HPLC method. *Folia Zool.* **2009**, *58*, 75–81.

25. Kozlik, P.; Bosakova, Z.; Tesarova, E.; Coufal, P.; Cabala, R. Development of a solid-phase extraction with capillary liquid chromatography tandem mass spectrometry for analysis of estrogens in environmental water samples. *J. Chromatogr. A* **2011**, *1218*, 2127–2132. [CrossRef] [PubMed]

26. Bosakova, T.; Tockstein, A.; Sebkova, N.; Simonik, O.; Adamusova, H.; Albrechtova, J.; Albrecht, T.; Bosakova, Z.; Dvorakova-Hortova, K. New insight into sperm capacitation: A novel mechanism of 17β-estradiol signalling. *Int. J. Mol. Sci.* **2018**, *19*, 4011. [CrossRef] [PubMed]

27. Bosakova, Z.; Tockstein, A.; Adamusova, H.; Coufal, P.; Sebkova, N.; Dvorakova-Hortova, K. Kinetic analysis of decreased sperm fertilizing ability by fluorides and fluoroaluminates: A tool for analyzing the effect of environmental substances on biological events. *Eur. Biophys. J.* **2016**, *45*, 71–79. [CrossRef]

28. Davis, B.K.; Byrne, R.; Hungund, B. Studies on the mechanism of capacitation. II Evidence for lipid transfer between plasma membrane of rat sperm and serum albumin during capacitation in vitro. *J. Chromatogr. B* **1979**, *558*, 257–266. [CrossRef]

29. Dow, M.P.D.; Bavister, B.D. Direct contact is required between serum albumin and hamster spermatozoa for capacitation in vitro. *Gamete Res.* **1989**, *23*, 171–180. [CrossRef]

30. Romeu, A.M.; Martino, E.E.; Stoppani, A.O. Structural requirements for the action of steroids as quenchers of albumin fluorescence. *Biochim. Biophys. Acta* **1975**, *409*, 376–386. [CrossRef]

Kinetic Study of 17α-Estradiol Activity in Comparison with 17β-Estradiol and 17α-Ethynylestradiol

Tereza Bosakova [1,2], Antonin Tockstein [1], Zuzana Bosakova [1,*] and Katerina Komrskova [2,3,*]

[1] Department of Analytical Chemistry, Faculty of Science, Charles University, Albertov 2030, 128 43 Prague 2, Czech Republic; tereza.bosakova@natur.cuni.cz (T.B.); atockstein@seznam.cz (A.T.)

[2] Laboratory of Reproductive Biology, Institute of Biotechnology, Czech Academy of Sciences, BIOCEV, Prumyslova 595, 252 50 Vestec, Czech Republic

[3] Department of Zoology, Faculty of Science, Charles University, Vinicna 7, 128 44 Prague 2, Czech Republic

* Correspondence: bosakova@natur.cuni.cz (Z.B.); katerina.komrskova@ibt.cas.cz (K.K.); Tel.: +420-2219-51231 (Z.B.); +420-6048-55871 (K.K.)

Abstract: 17α-estradiol (αE2), an endogenous stereoisomer of the hormone 17β-estradiol (E2), is capable of binding to estrogen receptors (ER). We aimed to mathematically describe, using experimental data, the possible interactions between αE2 and sperm ER during the process of sperm capacitation and to develop a kinetic model. The goal was to compare the suggested kinetic model with previously published results of ER interactions with E2 and 17α-ethynylestradiol (EE2). The HPLC-MS/MS method was developed to monitor the changes of αE2 concentration during capacitation. The calculated relative concentrations B_t were used for kinetic analysis. Rate constants k and molar ratio n were optimized and used for the construction of theoretical $B(t)$ curves. Modifications in αE2–ER interactions were discovered during comparison with models for E2 and EE2. These new interactions displayed autocatalytic formation of an unstable adduct between the hormone and the cytoplasmic receptors. αE2 accumulates between the plasma membrane lipid bilayer with increasing potential, and when the critical level is reached, αE2 penetrates through the inner layer of the plasma membrane into the cytoplasm. It then rapidly reacts with the ER and creates an unstable adduct. The revealed dynamics of αE2–ER action may contribute to understanding tissue rejuvenation and the cancer-related physiology of αE2 signaling.

Keywords: 17α-estradiol; 17β-estradiol; 17α-ethynylestradiol; estrogen receptors; sperm; capacitation; HPLC MS/MS; kinetics; autocatalysis

1. Introduction

Estrogens are steroid hormones, and if present in the environment, they are classified as pollutants called endocrine-disrupting chemicals (EDCs) [1]. Even at extremely low concentrations (ng/L) they can have a detrimental impact on the endocrine systems of animals, including humans. EDCs can simulate the behavior of endogenous estrogens, which control several physiological processes, including male reproduction and in particularly sperm maturation [1–4].

An interaction between estrogens and their estrogen receptors (ER) has been characterized not only through nuclear receptors (nER) but also membrane (mER) and cytoplasmic (cER) receptors [5,6]. Several estrogenic hormones also lead to an increase in germ cell apoptosis and a decrease in sperm count [7,8]. It is therefore vital to study estrogens and ER interactions because they are heavily involved in the sperm maturation process called capacitation. It is during capacitation that sperm gain the capacity to fertilize the egg. We developed a novel approach utilizing the kinetic analysis of experimental data using theoretical modelling that resulted in new perspectives and interpretation of data.

Basic estrogens include the endogenous and biologically most active hormones 17β-estradiol (E2), 17α-estradiol (αE2) estriol (E3), estrone (E1) as well as synthetic 17α-

ethynylestradiol (EE2), used in hormonal contraceptives [9]. αE2 is the natural stereoisomer of E2 present endogenously. Its biological activity ranges between 1.5 and 5% of E2 activity with respect to species and tissue specificity [10–12]. It has recently been found to prolong the life of male mice, and to block inflammatory disfunction [10,13]. It has been discovered that αE2 is capable of binding to both ERα and ERβ receptors, both of which are present on the sperm plasma membrane (genomic effect). This is like the behavior of E2, but with much lower affinity [14]. In addition, αE2 can bind to cerebral ER-X receptors and membrane-associated plasma receptors (non-genomic effect) [15]. This can, for example, be manifested in a relaxation of the uterine smooth muscles [16]. αE2 has also been detected in small concentrations in samples of human urine and serum [17]. The responsiveness of male mice, but not castrated males or females, to αE2 treatment suggests sex specificity in the responses to αE2. This is caused by an interaction with male gonadal hormones, for example, the production of testosterone [18]. αE2 has a range of bioactive properties, including inflammatory and antioxidant effects [19] and an ability to inhibit the activity of 5α-reductase enzymes [20], which convert testosterone to dihydrotestosterone—a more potent activator of the androgen receptor. αE2 has been studied to demonstrate its benefit in the modulation of ovariectomy-mediated obesity and bone loss [21]. Treatment of male mice with αE2 has been shown to extend median lifespan [10,13,18,22]. It also improved male glucose tolerance during most of the adult life [23,24]. However, the mechanisms by which αE2 provides these benefits remain a matter of debate, even if αE2 elicits similar genomic binding and transcriptional activation through estrogen receptors to that of E2 [25].

The biological and physical processes that sperm undergoes after ejaculation are known as *capacitation* [26]. Only capacitated sperm gain progressive motility (sperm hyperactivation) and are capable of penetrating through the egg envelope (in a process known as the *acrosome reaction*) and to subsequently fertilize the egg [27]. Capacitation in vivo includes several fundamental processes: an increase in the liquidness of the cytoplasmic membrane; a reduction in cholesterol concentration in the membrane (termed cholesterol efflux); the opening of ion channels followed by a change in membrane potential; the loss of some surface proteins (and phosphorylation of proteins leading to hyperactivation); and the *acrosome reaction* [28]. It is significant that EDCs can affect all these physiological processes and modify their interactions [4].

To study capacitation, the process needs to be simulated in vitro and must fulfil strict requirements regarding sperm incubation. This includes a capacitation/fertilization medium containing albumin and calcium ions at a temperature of 37 °C, maintained in an atmosphere with 5% CO_2. These specific conditions imitate the physiological environment in the female genital tract [29]. To study how the presence of estrogens effect sperm capacitation in vitro, it is important to determine the capability of sperm to bind these hormones and the dynamics of this process. By using kinetic analysis on experimental data, we may be able to resolve this process. A similar approach has already been used to monitor time-dependent changes in mRNA concentration [30,31].

The developed HPLC-MS/MS methods enabled monitoring of the concentration changes of the free, unbound hormone (E2 or EE2) during time-dependent capacitation of mouse sperm (dose concentrations 200, 20 and 2 μg/L). Then, this was achieved through the dependence of the relative concentration of the free hormone (*B*) on capacitation time (*t*) [32,33]. It was apparent from the shape of the *B(t)* curves, obtained for previously studied E2 or EE2, that the hormones form unstable adducts with the receptors and that the formation of these adducts acts autocatalytically [32,33]. It was therefore hypothesized that analogous behavior could also be occurring for the interaction between αE2 and ER in maturing sperm.

This research was performed to determine whether the action of αE2 during the capacitation of mouse sperm exhibits a similar pattern to that of E2 and EE2 [32,33]. Firstly, to answer this question, we developed an HPLC-MS/MS method capable of monitoring the concentration changes of unbound free αE2 during the time-dependent capacitation of

mouse sperm (in a capacitation M2 medium). Secondly, we subjected the obtained results to kinetic analysis. To make a valid comparison between αE2 and previously measured hormones E2 and EE2, the following parameters were kept constant: measurement methodology; concentrations of hormone; evaluation of the obtained data for kinetic analysis; and mathematical procedure.

2. Results

2.1. Monitoring the αE2 Concentration during Time-Depedent Capacitation Using the HPLC-MS/MS Method

Similar to a previous study of the concentration changes in the estrogenic hormones E2 [32] and EE2 [33] during the time-dependent capacitation of mouse sperm, the HPLC-MS/MS method was selected for an analogous study of the estrogenic hormone αE2. As a first step, under optimized separation and capacitation conditions (see Chapter 4.2), the concentration of free unbound αE2 (dependent on the capacitation time) was monitored for a dose concentration of 200 μg/L. The resultant data are shown in Figure 1. It is apparent from these data that sample values first decreased to a capacitation time of 150 min, where they attained a minimum, and thereafter increased. In contrast, the blank values remained essentially constant during the whole capacitation time. For dose concentrations of 20 and 2 μg/L, the samples exhibited practically no difference compared to the blank and almost constant values that were obtained for all the monitored capacitation times, varying in intervals from 17.8 to 18.6 μg/L for dose concentrations of 20 μg/L and from 1.7 to 1.8 μg/L for the dose concentration of 2 μg/L.
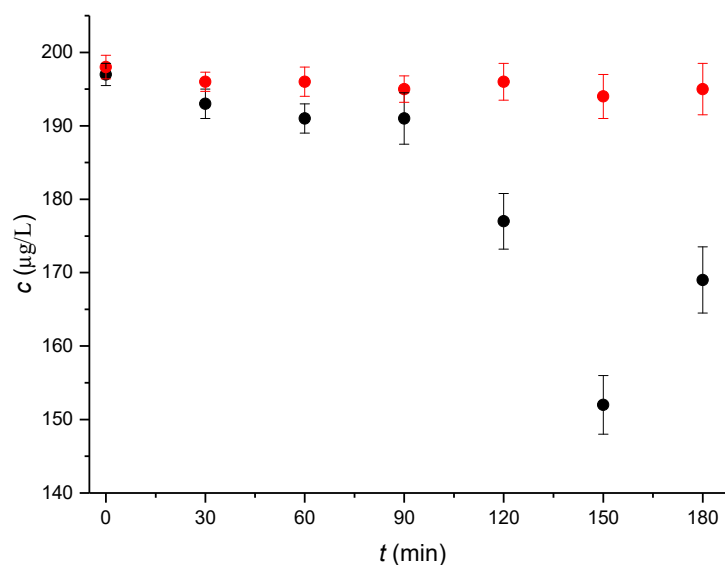

Figure 1. Dependences of the concentration of total unbound αE2 on the time of mouse sperm capacitation in vitro. The tested concentration of αE2 in capacitating medium was 200 μg/L. The samples were prepared in three parallel sets, where each set represented sperm collected from one individual (black dots). The blanks were prepared and measured in parallel (red dots). Experimental conditions: 50/50 (*v*/*v*) ACN/H_2O, both containing 0.1% HCOOH, were measured in the multiple reaction monitoring (MRM) mode for transition 255.0→158.9, and the error bars were calculated using the standard deviations ($n' = 3$) according to the methodology used for E2, EE2 hormones [32,33].

The measured values for a dose concentration of 200 μg/L yielded the values of the relative concentration B_t defined as $C(t)/C(t = 0)$ for the individual capacitation times. The relevant values are given in Table 1.

Table 1. Relative concentrations (B_t) calculated from the means of measured αE2 time-dependent concentrations C ($n' = 3$) obtained during capacitation for the tested concentration of 200 μg/L αE2 (see Figure 1); mean $\pm$ standard error of the mean.

Time (min)	0	30	60	90	120	150	180
B_t	1.000 ± 0.002	0.985 ± 0.002	0.981 ± 0.003	0.979 ± 0.008	0.899 ± 0.010	0.772 ± 0.012	0.863 ± 0.013

The B_t values of the samples and blank obtained for the dose concentration of 20 μg/L oscillated around 0.957 and for the dose concentration of 2 μg/L around 0.944. Due to their constant values throughout the capacitation time, they were not involved in further kinetic studies.

2.2. Kinetic Analysis of the HPLC-MS/MS Data

If a curve is fitted through the experimentally obtained values of B_t, it might at first appear that this curve has a similar shape to the one obtained from the experimentally obtained B_t values of the previously studied E2 and EE2 hormones. In our previous research targeting the E2 and EE2 reaction with ER in mouse sperm during sperm capacitation, it was found that both E2 and EE2 display a common characteristic in the autocatalytic formation of an unstable adduct between the relevant hormone (E2 or EE2) and the estrogen receptors (cER) located in the cytoplasm, and this was manifested by a decrease followed by an increase in the B_t value [32,33].

Based on the published data for EE2 [33], the decomposition of the adduct could be described by two hypothetical possibilities that could also apply for αE2: (a) decomposition produces active estrogen hormone and active R (cER) receptor, which are both capable of further interactions; (b) the decomposition produces active estrogen hormone and inactive receptor R$'$, incapable of further interaction. Because both components formed in the first reaction (a) are hypothetically active, it is simple to imagine a reverse (equilibrium) reaction between the hormone and the estrogen receptor R in the cytoplasm. On the other hand, the second reaction (b) is a unidirectional leading to a deactivation of the receptor. These two reactions (a) and (b) could take place simultaneously and this phenomenon can be considered as a disturbance of the equilibrium (i.e., a pseudo-equilibrium reaction). The process observed for αE2 together with the set of equations can be described by the following simple kinetic scheme (see Figure 2).
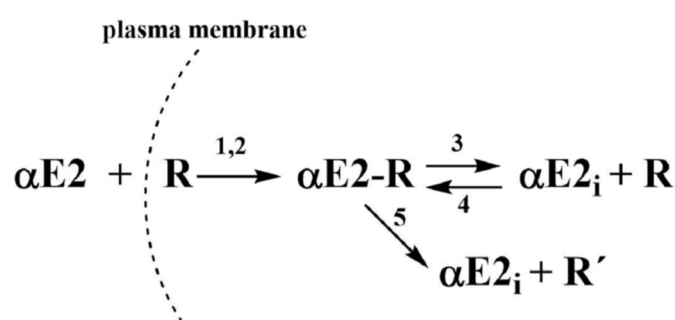

Figure 2. Kinetic scheme where: αE2 is the extracellular hormone; R is the active sperm receptor; αE2-R is the adduct; αE2$_i$ is the internal free hormone and R' is the inactive sperm receptor. The plasma membrane is not a flat surface but is an intermediate phase with an external orientation facing the hormone solution, and an internal orientation facing the cytoplasm. 1 and 2 represent rate constants of non-autocatalytic (1) and autocatalytic (2) formation of αE2-R, ongoing simultaneously; 3 and 5 represent rate constants of adduct decomposition, and 4 represents a rate constant of reverse reaction.

Based on the scheme in Figure 2, the monitoring of αE2 concentration by HPLC/MS-MS is related to the overall concentration of free, unbound hormone, i.e., the original αE2 and the internal αE2$_i$. After centrifugation, both components of the hormone were present

in the supernatant. However, the hormone bound in the complex with the receptor (adduct: αE2-R) remains in the sediment and its concentration was not measured.

Additionally, the kinetic scheme employs kinetic products and rate constants in the form of differential equations. For brevity, the term αE2 is replaced in the equations by the symbol *E* (also designating its molar concentration under various experimental conditions), *R* designates the cytoplasmic estrogen receptor (cER) and its concentration, symbol (*ER*) designates the adduct, E_i is the internal free hormone in the cytoplasmic membrane, and R' is the inactive cER receptor.

$$\frac{-\mathrm{d}E}{\mathrm{d}t} = E \times R(K_1 + K_2 \times (1 - \varepsilon)) \tag{1}$$

$$\frac{-\mathrm{d}R}{\mathrm{d}t} = E \times R(K_1 + K_2 \times (1 - \varepsilon)) + K_4 \times E_i \times R - K_3 \times (ER) \tag{2}$$

$$\frac{\mathrm{d}(ER)}{\mathrm{d}t} = E \times R(K_1 + K_2 \times (1 - \varepsilon)) + K_4 \times E_i \times R - (K_3 + K_5) \times (ER) \tag{3}$$

Equation (1) describes the decrease in the hormone *E* by a reaction with the receptor *R*. Equation (2) describes the decrease in the receptor through its reaction with the external and internal pool of the hormone and the increase by the subsequent adduct decomposition. Equation (3) describes the increase in the adduct through the autocatalytic reaction and reverse reaction including the decrease through the equilibrium (K_3) and pseudo-equilibrium (K_5) reactions.

These differential equations were subsequently solved by the Runge–Kutta method, used to determine the values of the parameters of the theoretical $B(t)$ curve, i.e., the rate constants K_1–K_5 and the value of the molar ratio of the reacting components, parameter *n*. These values were optimized by looking for the minima in the absolute values of the difference between the theoretical and experimental B_t values using the MATLAB program. The results of optimization of the rate constants and parameter *n* for a concentration of 200 µg/L are listed in Table 2. The derivation of the individual differential equations and reasons for their specific position are described in Reference [33].

Table 2. Calculated constants obtained for an αE2 concentration of 200 µg/L, where K_1–K_5 are the overall rate constants and *n* is the molar ratio.

K_1	K_2	K_3	K_4	K_5	*n*
0.01	4.0	5.0	0	0	0.01

The $B(t)$ curves formed using constants K_1–K_5 for the various values of the parameter *n* are given in Figure 3. The way in which the shape and position of the minima of the $B(t)$ curves depend on the value *n* is apparent from the shapes of the individual curves. It is evident that the fitting of the experimentally obtained points (black points) with the minimum of the calculated $B(t)$ curve is tighter for extremely small *n* values (red or green points).

As mentioned above, the shape and form of the $B(t)$ curve for αE2 might initially appear to agree with the $B(t)$ curve (obtained for the reaction of the previously studied EE2 hormone [33]), corresponding to the autocatalytic formation of an unstable adduct. However, important differences in the results necessitate the development of a different reaction mechanism. The most significant differences between the αE2 and EE2 data are as follows:

(i)   The initial branch of the hypothetical curve that would be obtained by fitting the experimental points is the opposite to that of the autocatalytic curve.

(ii)   The slope of the tangent to this hypothetical curve decreases in its initial region to zero with time.

(iii) The determined value of *n* is too low for a dose hormone concentration of 200 µg/L.
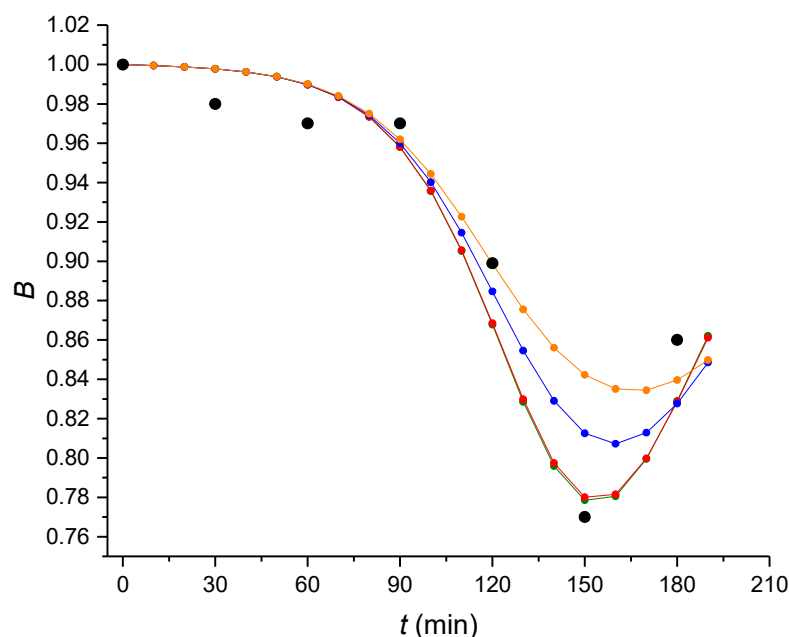
Figure 3. Shape of the theoretical $B(t)$ curves calculated with optimized K_1–K_5 constants (see Table 2) for various values of the molar ratio *n*: 0.01—green line; 0.1—red line; 1—blue line; 2—orange line; experimentally obtained B_t values—black dots.

As a result, further optimization of the rate constants was performed to enable a better fitting of the experimental points obtained during a capacitation time of 0–90 min, and the resultant data can be found in Table 3.

Table 3. Calculated constants obtained for an αE2 concentration of 200 μg/L, where K_1–K_5 are the overall rate constants and *n* is the molar ratio.

K_1	K_2	K_3	K_4	K_5	*n*
7	10	49	12	20	0.01

Figure 4 gives the experimentally determined values of B_t (black dots) together with the curves obtained using the optimized kinetic constants given in Table 2 (Curve 1) and Table 3 (Curve 2). The initial branch of Curve 2 up to the intersection with Curve 1 (at 90 min of capacitation), corresponds to the difficulty of the αE2 hormone finding an entrance into the external facing surface of the plasma membrane. αE2 does not initially pass through the inner facing layer of the plasma membrane and it accumulates with increasing strain between the plasma membrane lipid bilayer. When the amount of αE2 in the plasma membrane reaches a critical value, the inner layer of the membrane becomes permeable for αE2. This results in the internalization of αE2 within the cytoplasm, where the hormone rapidly reacts autocatalytically with the estrogen receptor (cER) and forms an unstable adduct (note the sharply decreasing branch of Curve 1), which subsequently decomposes (see the final, increasing branch of Curve 1). The described process results in a $B(t)$ angled curve. Because the critical amount of αE2 is extremely low relative to the total content of cER in the cytoplasm, the value of the parameter *n* is extremely low in the reaction of the hormone with the cytoplasm receptors.
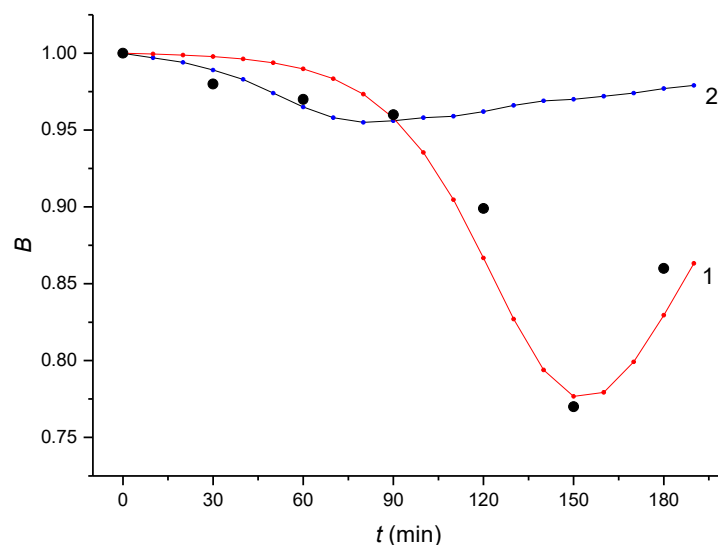
Figure 4. The values of the relative concentration B_t obtained experimentally by the HPLC/MS/MS method (black dots) together with the theoretically calculated $B(t)$ curves obtained by integration of the kinetic equations with optimized constants given in Table 2 (Curve 1) and Table 3 (Curve 2). The dose concentration of αE2 was 200 μg/L.

The initial branch of Curve 1 should be much slower for a concentration of 20 μg/L (or 2 μg/L) compared to a concentration of 200 μg/L, so the minimum should occur after 180 min. Significantly, this is after the standard capacitation time. This theory is confirmed by the experimental findings.

3. Discussion

From the kinetic analysis of experimentally determined values of the relative concentration (B_t) for individual capacitation times, the results show that one uniform process resulted in the formation of an adduct formed by the hormones (E2, EE2, αE2) and the sperm cytoplasmic estrogen receptor (cER). The formed adducts are unstable and decompose to the original free hormones (E2, EE2, αE2) and cER [32,33]. If the decomposition results in an unaltered receptor (that can react with the internal pool of the hormone to form the adduct by a reverse reaction), then this is defined as an equilibrium reaction. If an inactive receptor is present, then the equilibrium reaction is interrupted and leads to a pseudo-equilibrium reaction.

The formation of the adduct is an autocatalytic reaction characterized by the fact that the tangent to the $B(t)$ curve becomes steeper during the reaction. The autocatalysis consists of the formed adduct that relaxes the plasma membrane and facilitates a passage of the hormones (E2, EE2, αE2) with increased production of the adduct. This process is then repeated. Based on the outcome of kinetic analysis, the difference in the response of the individual hormones appears to be due to a different mode of transport of the hormones through the plasma membrane.

E2 is an endogenic hormone that requires defined membrane estrogen receptors to generate the required response. The number of receptors on the surface of sperm is determined by the adsorption isotherm. E2 can only penetrate through the plasma membrane to form the adduct through the receptors. Because the isotherm is proportional to the concentration of the external E2 hormone; the formation of the adduct is also dependent on the same process. The minimum value on the time axis is an important element on the $B(t)$ curves and is dependent on the dose hormone concentration. Specifically, the minimum shifts to later capacitation times as the dose hormone concentration decreases [32]. This result clearly indicates that an endogenic hormone is involved. The depth of the minimum on the $B(t)$ curve deepens as the value of n (molar ratio) decreases. The ratio of the two neighboring n_1/n_2 values obtained for two neighboring dose concentrations ((200;

20 µg/L) or (20; 2 µg/L)), equals 1/10, and this is in accordance with the ratio of two neighboring dose concentrations. It represents another typical characteristic behavior of the E2 hormone [32]. However, the described kinetic action for the E2 hormone was not the case for the other estrogen hormones.

The experimentally determined n values for the individual dose concentrations are much smaller for the EE2 than the corresponding n values for E2. The EE2 hormone does not seem to require a specific membrane estrogen receptor to pass through the sperm plasma membrane and therefore this reaction is rapid. A characteristic feature of the EE2 action is the fact that the time coordinates of the minimum are practically constant and, therefore, they are independent of the hormone dose concentration [33].

The passage through the plasma membrane is substantially more complicated for the αE2 hormone. Firstly, αE2 does not appear to pass through the inner facing layer of the plasma membrane and it accumulates between the plasma membrane lipid bilayer. It is manifested by the relatively long, flat part of the $B(t)$ curve. When the amount of αE2 within the plasma membrane reaches a critical value, the inner layer of the membrane becomes permeable for αE2, followed by internalization of αE2 within the cytoplasm. Here, the hormone rapidly reacts autocatalytically with cytoplasmic receptors and forms an unstable adduct, demonstrated by a sharp decrease in the $B(t)$ curve to the minimum point. The critical amount of this hormone is small compared to the overall amount of estrogen receptors in the sperm cytoplasm. The value of parameter n is also extremely low in the reaction of the hormone with the cER. It is important to note that the kinetic model suggested for αE2 (a hormone with low hormonal activity) is successfully described by the same differential equations as EE2 that represent a synthetic hormone. These conclusions support the validity of the proposed kinetic models. Suggested mathematical models, validated by experimental data, allowed for the development of hypotheses for possible interactions between estrogen hormones and estrogen receptors using the sperm capacitation model.

αE2 has also been discovered to bind to brain-expressed ER-x [15] and breast-expressed ER-X [34] membrane-associated receptors to mediate estrogen-specific signaling and classical ER [6]. These receptors have a sequence homology to ER which is known to be expressed in gonads including sperm. However, the role of these receptors in male reproduction remains to be determined [6,35]. It is of importance that αE2 was described to be biologically active in human breast cancers [11]. Since testicular germ cell cancer (TGCT) is associated with polymorphism in estrogen receptors and steroid metabolism genes, sex steroid action is regarded as involved in the development of TGCT [36]. As estrone (E1) is metabolized to estradiol (E2), there is a strong correlation with functional activity, estradiol level, or estrogen-related outcomes between TGCT [37] and breast cancer [11]. αE2 represents the endogenous estradiol isomer for which biological roles are described but not fully understood. αE2 is shown to play a crucial role in regenerating brain tissue after injury [38,39], and its significant role in cancer-related events including TGCT has been published. The novel understanding of the dynamics of αE2–ER crosstalk on the sperm model presented in this paper has the potential to be used for advanced understanding of the physiology of its signaling action within cells.

4. Materials and Methods

In order to guarantee the comparison between studied hormones, relevant materials and methods were used according to previously published kinetic studies [32,33]. The Materials and Methods section was updated to include αE2.

4.1. Chemicals, Reagents and Animals

Acetonitrile (ACN) for LC-MS, Chromasolv (purity ≥ 99.9%), deuterated β-estradiol-16,16,17-d3 (estradiol-d3) (purity 98%), and commercial capacitating M2 culture media for in vitro sperm capacitation and fertilization (M7167) were purchased from Sigma-Aldrich (Steinheim, Germany). Ethanol (purity ≥ 96% p.a.) was obtained from Lachner (Neratovice,

Czech Republic). Paraffin oil was provided by Carl Roth (Karlsruhe, Germany). Formic acid (HCOOH) (LC-MS LiChropur, purity 97.5–98.5%), 17α-estradiol (purity 98%) and deionized water (for UHPLC-MS LiChrosolv) were obtained from Merck (Darmstadt, Germany).

The laboratory inbred house mouse strain BALB/c was used for the experiments. The mice were housed in the animal facilities of the Institute of Molecular Genetics of the Czech Academy of Science, Prague. Food and water were supplied ad libitum. All the animal procedures and all the experimental protocols were approved by the Animal Welfare Committee of the Czech Academy of Sciences (Animal Ethics Number 66866/2015-MZE-17214, 18 December 2015).

4.2. Instrumentation and Chromatographic Conditions

The HPLC equipment (Agilent Technologies, Waldbronn, Germany) consisted of 1290 Infinity Series LC (a quaternary pump, degasser, thermostatic auto sampler and column oven). A Triple Quad LC/MS 6460 tandem mass spectrometer (Agilent Technologies, Waldbronn, Germany) with an electrospray ionization interface was used for the detection. The signal was processed, and the data were retreated using the MassHunter Workstation Acquisition and MassHunter Qualitative Analysis Software (Agilent Technologies, Waldbronn, Germany).

All the instrumental MS-MS parameters were optimized. The ESI (+) conditions in the MRM mode for αE2 were capillary voltage 4000 V, nebulizer pressure 55 psi, gas temperature 350 °C, and a nitrogen flow rate of 10 L/min.

For αE2, the *m/z* 255.0→158.9 and for estradiol-d3, the *m/z* 258.5→158.9 transitions were monitored (fragmentor voltage 130 V, collision energy 14 V, parameter dwell 200 ms).

The separation system was based on publications [33,40] with a Kinetex EVO column C18 (100 × 3.0 mm, 2.6 μm, Phenomenex, Torrance, CA, USA) and a mobile phase containing a binary mixture of ACN/water with the addition of 0.1% HCOOH in both parts at a volume ratio of 50/50 (*v/v*); the flow rate was 0.3 mL/min. The column temperature was held at 21 ± 0.5 °C. The amount of sample injected equaled 7.5 μL. Estradiol-d3 was added to each sample as an internal standard (IS) at a final concentration of 25 μg/L (diluted in the capacitating medium). The retention times of IS and αE2 were 3.0 and 3.4 min, respectively. Because of the complex capacitating medium containing inorganic and organic components, of which especially bovine serum albumin (4.0 g/L) can cause difficulties during the separation and detection processes, the eluate was fed to waste from 0 to 2.5 min and to the MS detector only from 2.5 to 5 min.

The linearity of the method was determined from the calibration curve constructed by plotting the ratio of the peak areas of αE2 to that of IS against the analyte concentration. It was statistically analyzed by 1/x weighted linear regression analysis using the least-squares regression method. The obtained data were linear (y = 0.0544x + 0.0702, R^2 = 0.9987) in the whole measured calibration range 1–250 μg/L. Relative standard deviations (*n* = 5) varied from 1.8–5.9%. The limit of detection (0.52 μg/L) and limit of quantitation (1.49 μg/L) were calculated as the $3.3 \times \sigma/S$ and $10 \times \sigma/S$ ratios, respectively, where σ was the baseline noise of the sample and *S* was the slope of the regression curve (based on the ratio of the peak heights of αE2 to that of IS against the analyte concentration) constructed from the calibration curve.

4.3. Sample Preparation

35 mM culture dishes purchased from Corning (Corning, NY, USA) were used for the capacitation in vitro. The Olympus CX 21 inverted-light microscope and Olympus epifluorescent microscope were supplied by Olympus (Prague, Czech Republic). The NB-203 incubator was purchased from N-BIOTEK (Gyeonggi-do, Korea). The Telstar Bio-IIA incubator and BioTek laminar box from N-BIOTEK (Gyeonggi-do, Korea) were used for the in vitro sperm cultivation.

First, a stock solution of the αE2 standard with a concentration of 200 mg/L was prepared in ethanol, from which the working ethanol solutions of an αE2 concentration of

20 and 2 mg/L were diluted. In the laminar box, 10 μL of the working ethanol solution of αE2 with the appropriate concentration (200, 20 or 2 mg/L) was pipetted and diluted with capacitating medium to a volume of 10 mL in the test tube, so that the final test concentration of αE2 in the capacitating medium was obtained (200, 20 or 2 μg/L) and the ethanol content was minimized and remained constant. Subsequently, 100 μL of solution with the appropriate concentration was pipetted into the fertilization Petri dish. The pipetted mixture in the Petri dish was covered with 1 mL of paraffin oil. The prepared Petri dishes were placed in the incubator and tempered for 60 min at a temperature of 37 °C and with 5% CO_2 in the air.

The spermatozoa which were recovered from the distal region of the *cauda epididymidis* were placed in fertilization Petri dishes with a capacitating medium and paraffin oil and then placed for 10 min in the incubator for sperm release. Next, the stock concentration of mouse sperm was adjusted to 5×10^6 sperm/mL. The control experiments monitoring sperm motility and viability were run in parallel and controlled under a microscope. No toxicological effect of αE2 in capacitation media was found.

The biological sample was prepared as follows: following 60 min of tempering, 5 μL of the stock sperm was added to 100 μL of the αE2 sample in capacitating medium (200, 20 or 2 μg/L). For each capacitation time (0–180 min), 8 Petri dishes containing 105 μL of sample covered with 1 mL of paraffin oil were prepared. The dishes prepared in this way were incubated again under the same conditions for various time periods (0, 30, 60, 90, 120, 150 and 180 min after adding the sperm), during which sperm capacitation took place. After the individual times, samples (only the solution with the capacitating medium, without the paraffin oil) were pipetted from all 8 Petri dishes into a single micro-test tube, which was centrifuged for 10 min at 12,000 rpm. In this way, the sperm were separated from the solution and approximately 600 μL of supernatant was obtained for HPLC-MS/MS analysis of free, sperm unbound αE2. This sample represented one sampling time during capacitation.

In order to eliminate any systematic errors during sample preparation (partial evaporation of samples during incubation, differences in collection of supernatants after centrifugation, etc.), reference samples (blanks) without the addition of mouse sperm were prepared simultaneously under the same experimental conditions.

Prior to the actual HPLC-MS/MS analysis, 20 μL of IS (estradiol-d3) with a concentration of 250 μg/L was added to each biological sample as well as to a blank (180 μL).

The matrix effect was investigated by a comparison of results (αE2/IS peak area ratios) obtained for samples prepared by two different procedures: (i) the sample was prepared by the addition of αE2 and IS to the supernatant, obtained after the capacitating medium with sperm covered with paraffin oil was tempered, the paraffin oil removed and capacitating medium centrifuged; (ii) the sample was prepared by addition of αE2 and IS to the capacitating medium. Each experiment was performed in triplicate for concentrations of 200, 20 and 2 μg/L. The recovery of the samples with αE2 was 96.8% for 200 μg/L, 98.5% for 20 μg/L and 91.3% for 2 μg/L.

References

1. López de Alda, M.J.; Barceló, D. Determination of steroid sex hormones and related synthetic compounds considered as endocrine disruptors in water by liquid chromatography-diode array detection-mass spectrometry. *J. Chromatogr. A* **2000**, *892*, 391–406. [CrossRef]
2. Colborn, T.; vom Saal, F.S.; Soto, A.M. Developmental effects of endocrine-disrupting chemicals in wildlife and humans. *Environ. Health Perspect.* **1993**, *101*, 378–384. [CrossRef] [PubMed]
3. Della Seta, D.; Farabollini, F.; Dessí-Fulgheri, F.; Fusani, L. Environmental-like exposure to low levels of estrogen affects sexual behavior and physiology of female rats. *Endocrinology* **2008**, *149*, 5592–5598. [CrossRef] [PubMed]
4. Hess, R.A. Estrogen in the adult male reproductive tract: A review. *Reprod. Biol. Endocrinol.* **2003**, *1*, 52. [CrossRef]
5. Aquila, S.; De Amicis, F. Steroid receptors and their ligands: Effects on male gamete functions. *Exp. Cell Res.* **2014**, *328*, 303–313. [CrossRef] [PubMed]
6. Dostalova, P.; Zatecka, E.; Dvorakova-Hortova, K. Of oestrogens and sperm: A review of the roles of oestrogens and oestrogen receptors in male reproduction. *Int. J. Mol. Sci.* **2017**, *18*, 904. [CrossRef] [PubMed]
7. Kumar, V.; Majumdar, C.; Roy, P. Effects of endocrine disrupting chemicals from leather industry effluents on male reproductive system. *J. Steroid Biochem. Mol. Biol.* **2008**, *111*, 208–216. [CrossRef] [PubMed]
8. Jensen, T.K.; Toppari, J.; Keiding, N.; Skakkebaek, N.E. Do environmental estrogens contribute to the decline in male reproductive health? *Clin. Chem.* **1995**, *41*, 1896–1901. [CrossRef] [PubMed]
9. LaFleur, A.D.; Schug, K.A. A review of separation methods for the determination of estrogens and plastics-derived estrogen mimics from aqueous systems. *Anal. Chim. Acta* **2011**, *696*, 6–26. [CrossRef]
10. Strong, R.; Miller, R.A.; Antebi, A.; Astle, C.M.; Bogue, M.; Denzel, M.S.; Harrison, D.E. Longer lifespan in male mice treated with a weakly estrogenic agonist, an antioxidant, an α-glucosidase inhibitor or a Nrf2-inducer. *Aging Cell* **2016**, *15*, 872–884. [CrossRef] [PubMed]
11. Edwards, D.P.; McGuire, W.L. 17 alpha-Estradiol is a biologically active estrogen in human breast cancer cells in tissue culture. *Endocrinology* **1980**, *107*, 884–891. [CrossRef]
12. Trüeb, R.M.; Lee, W.-S. *Male Alopecia: Guide to Successful Management*; Springer Science & Business Media: New York, NY, USA, 2014; p. 93.
13. Stout, M.B.; Steyn, F.J.; Jurczak, M.J.; Camporez, J.G.; Zhu, Y.; Hawse, J.R.; Jurk, D.; Palmer, A.K.; Xu, M.; Pirtskhalava, T.; et al. 17α-Estradiol alleviates age-related metabolic and inflammatory dysfunction in male mice without inducing feminization. *J. Gerontol. A Biol. Sci. Med. Sci.* **2017**, *72*, 3–15. [CrossRef]
14. Perez, E.; Liu, R.; Yang, S.H.; Cai, Z.Y.; Covey, D.F.; Simpkins, J.W. Neuroprotective effects of an estratriene analog are estrogen receptor independent in vitro and in vivo. *Brain Res.* **2005**, *1038*, 216–222. [CrossRef] [PubMed]
15. Toran-Allerand, C.D.; Guan, X.; MacLusky, N.J.; Horvath, T.L.; Diano, S.; Singh, M.; Tinnikov, A.A. ER-X: A novel, plasma membrane-associated, putative estrogen receptor that is regulated during development and after ischemic brain injury. *J. Neurosci.* **2002**, *22*, 8391–8401. [CrossRef] [PubMed]
16. Perusquía, M.; Navarrete, E. Evidence that 17alpha-estradiol is biologically active in the uterine tissue: Antiuterotonic and antiuterotrophic action. *Reprod. Biol. Endocrinol.* **2005**, *3*, 30. [CrossRef]
17. Sievernich, A.; Wildt, L.; Lichtenberg-Frate, H. In vitro bioactivity of 17α-estradiol. *J. Steroid Biochem. Mol. Biol.* **2004**, *92*, 455–463. [CrossRef] [PubMed]
18. Garratt, M.; Leander, D.; Pifer, K.; Bower, B.; Herrera, J.J.; Day, S.M.; Fiehn, O.; Brooks, S.V.; Miller, R.A. 17-α estradiol ameliorates age-associated sarcopenia and improves late-life physical function in male mice but not in females or castrated males. *Aging Cell* **2019**, *18*, 2. [CrossRef]
19. Moos, W.H.; Dykens, J.A.; Nohynek, D.; Rubinchik, E.; Howell, N. Review of the effects of 17α-estradiol in humans: A less feminizing estrogen with neuroprotective potential. *Drug Dev. Res.* **2009**, *70*, 1–21. [CrossRef]
20. Schriefers, H.; Wright, M.C.; Rozman, T.; Hevert, F. Inhibition of testosterone metabolism by 17-alpha-estradiol in rat liver slices. *Arzneimittelforschung* **1991**, *41*, 1186–1189.
21. Mann, S.N.; Pitel, K.S.; Nelson-Holte, M.H.; Iwaniec, U.T.; Turner, R.T.; Sathiaseelan, R.; Kirkland, J.L.; Schneider, A.; Morris, K.T.; Malayannan, S.; et al. 17α-Estradiol prevents ovariectomy-mediated obesity and bone loss. *Exp. Gerontol.* **2020**, *142*. [CrossRef] [PubMed]
22. Harrison, D.E.; Strong, R.; Reifsnyder, P.; Kumar, N.; Fernandez, E.; Flurkey, K.; Javors, M.A.; Lopez-Cruzan, M.; Macchiarini, F.; Nelson, J.F. 17-a-estradiol late in life extends lifespan in aging UM-HET3 male mice; nicotinamide riboside and three other drugs do not affect lifespan in either sex. *Aging Cell* **2021**. [CrossRef] [PubMed]
23. Garratt, M.; Bower, B.; Garcia, G.G.; Miller, R.A. Sex differences in lifespan extension with acarbose and 17-alpha estradiol: Gonadal hormones underlie male-specific improvements in glucose tolerance and mTORC2 signaling. *Aging Cell* **2017**, *16*, 1256–1266. [CrossRef] [PubMed]
24. Isola, J.V.V.; Zanini, B.M.; Sidhom, S.; Kopchick, J.J.; Bartke, A.; Masternak, M.M.; Stout, M.B.; Schneider, A. 17α-Estradiol promotes ovarian aging in growth hormone receptor knockout mice, but not wild-type littermates. *Exp. Gerontol.* **2020**, *129*. [CrossRef] [PubMed]

25. Mann, S.M.; Hadad, N.; Holte, M.N.; Rothman, A.R.; Sathiaseelan, R.; Mondal, S.A.; Agbaga, M.-P.; Unnikrishnan, A.; Subramaniam, M.; Hawse, J.; et al. Health benefits attributed to 17a-estradiol, a lifespan-extending compound, are mediated through estrogen receptor a. *eLife* **2020**, *9*. [CrossRef] [PubMed]

26. Visconti, P.E.; Bailey, L.; Moore, G.D.; Olds-Clarke, P.; Kopf, G.S. Capacitation of mouse spermatozoa. *Development* **1995**, *121*, 1129–1137. [CrossRef]

27. Suarez, S.S.; Pacey, A.A. Sperm transport in the female reproductive tract. *Hum. Reprod. Update* **2006**, *12*, 23–37. [CrossRef] [PubMed]

28. Naz, R.K.; Rajesh, P.B. Role of tyrosine phosphorylation in sperm capacitation/acrosome reaction. *Reprod. Biol. Endocrinol.* **2004**, *2*, 75–87. [CrossRef]

29. Yanagimachi, R. *The Physiology of Reprodution*; Knobil, E.J.D.N., Ed.; Raven Press: New York, NY, USA, 1994; pp. 189–317.

30. Palumbo, M.C.; Farina, L.; Paci, P. Kinetics effects and modeling of mRNA turnover. *WIREs RNA* **2015**, *6*, 327–336. [CrossRef]

31. Cao, D.; Parker, R. Computation modeling of eukaryotic mRNA turnover. *RNA* **2001**, *7*, 1192–1212. [CrossRef]

32. Bosakova, T.; Tockstein, A.; Sebkova, S.O.; Adamusova, H.; Albrechtova, J.; Albrecht, T.; Bosakova, Z.; Dvorakova-Hortova, K. New insight into sperm capacitation: A novel mechanism of 17β-estradiol signalling. *Int. J. Mol. Sci.* **2018**, *19*, 4011. [CrossRef]

33. Bosakova, T.; Tockstein, A.; Sebkova, N.; Cabala, R.; Komrskova, K. Kinetic model of the action of 17α-ethynylestradiol on the capacitation of mouse sperm, monitored by HPLC-MS/MS. *Catalysts* **2020**, *10*, 124. [CrossRef]

34. Kampa, M.; Notas, G.; Pelekanou, V.; Troullinaki, M.; Andrianaki, M.; Azariadis, K.; Kampouri, E.; Lavrentaki, K.; Castanas, E. Early membrane initiated transcriptional effects of estrogens in breast cancer cells: First pharmacological evidence for a novel membrane estrogen receptor element (ERX). *Steroids* **2012**, *77*, 959–967. [CrossRef] [PubMed]

35. Ded, L.; Sebkova, N.; Cerna, M.; Elyeinova, F.; Dostalova, P.; Peknicova, J.; Dvorakova-Hortova, K. In vivo exposure to 17beta-estradiol triggers premature sperm capacitation in cauda epidimis. *Reproduction* **2013**, *145*, 255–263. [CrossRef]

36. Rajpert-De Meyts, E. Developmental model for the pathogenesis of testicular carcinoma in situ: Genetic and environmental aspects. *Hum. Reprod. Update* **2006**, *12*, 303–323. [CrossRef]

37. Ferlin, A.; Ganz, F.; Pengo, M.; Selice, R.; Frigo, A.C.; Foresta, C. Association of testicular germ cell tumor with polymorphisms in estrogen receptor and steroid metabolism genes. *Endocr. Relat. Cancer* **2010**, *17*, 17–25. [CrossRef]

38. Lermontova, N.N.; P'chev, V.K.; Beznosko, B.K.; Van'kin, G.I.; Ivanova, T.A.; Koroleva, I.V.; Lukoyanova, E.A.; Mukhina, T.V.; Serkova, T.P.; Bachurin, S.O. Effects of 17 beta-estradiol and its isomer 17 alpha-estradiol on learning in rats with chronic cholinergic deficiency in the brain. *Bull. Exp. Biol. Med.* **2000**, *129*, 442–444. [CrossRef] [PubMed]

39. McClean, J.; Nuñez, J.L. 17alpha-Estradiol is neuroprotective in male and female rats in a model of early brain injury. *Exp. Neurol.* **2008**, *210*, 41–50. [CrossRef]

40. Kozlík, P.; Bosáková, Z.; Tesařová, E.; Coufal, P.; Čabala, R. Development of a solid-phase extraction with capillary liquid chromatography tandem mass spectrometry for analysis of estrogens in environmental water samples. *J. Chromatogr. A* **2011**, *1218*, 2127–2132. [CrossRef]